Angewandte Chemie
Eine Zeitschrift der Gesellschaft Deutscher Chemiker

Supporting Information

Active in Sleep: Iron Guanidine Catalyst Performs ROP on Dormant Side of ATRP

*Ruth D. Rittinghaus, Aylin Karabulut, Alexander Hoffmann, and Sonja Herres-Pawlis**

anie_202109053_sm_miscellaneous_information.pdf

Table of Contents

Experimental Procedures

General

All steps were performed under nitrogen (99.996%), which was dried with P_4O_{10} granulate, using Schlenk techniques. Solvents were dried according to literature and stored under nitrogen.[1] All chemicals were purchased from Sigma-Aldrich GmbH, TCI GmbH, Thermo Fisher (Kandel) GmbH and ABCR GmbH and were used without further purification. L-lactide was donated by Total Corbion PLA and was used recrystallized once from dried toluene and subsequently sublimed under vacuo for copolymerizations. Lactide was stored at -35 °C in a nitrogen filled glovebox. IR spectra were measured with a Thermo Scientific Nicolet Avatar 380 spectrometer with a resolution of 2 cm^{-1}. The samples were prepared as KBr pellets. Elemental analysis was conducted with an *elementar varioEL*.

NMR spectrometry

NMR spectra were recorded at room temperature on a Bruker Avance II (400 MHz) or a Bruker Avance III (400 MHz). The NMR signals were calibrated to the residual signals of the deuterated solvent [$\delta_H(CDCl_3) = 7.26$ ppm, $\delta_C(CDCl_3) = 77.16$ ppm]. Data for ^{1}H NMR are reported as follows: chemical shift (δ ppm) (multiplicity, coupling constants (Hz), integration). Couplings are expressed by: s = singlet, d = doublet, m = multiplet or combinations thereof. ^{13}C NMR spectra are also expressed in parts per million (ppm) and reported as aforementioned. Various 2D NMR experiments (COSY, HSQC, HMBC, DEPT135) were used to assign the ^{1}H and ^{13}C NMR spectra of the ligand, DOSY NMR was performed for polymer characterization.

Gel permeation chromatography (GPC)

The average molecular masses and the mass distributions of the obtained polylactide samples were determined by GPC in THF as the mobile phase at a flow rate of 1 mL min^{-1}. The utilized GPCmax VE-2001 from Viscotek was a combination of an HPLC pump, two Malvern Viscotek T columns (porous styrene divinylbenzene copolymer) with a maximum pore size of 500 and 5000 Å, a refractive index detector (VE-3580), and a viscometer (Viscotek 270 Dual Detector). Conventional calibration with polystyrene was applied to evaluate the chromatographic results, molar masses of the copolymers are therefore given in polystyrene equivalents.

Complex synthesis and characterization

The ligand methyl 2-((bis(dimethylamino)methylene)amino)benzoate (TMGasme) was synthesized after known procedures from literature.[2] Complex synthesis was conducted in a nitrogen filled glovebox. Anhydrous iron(II) bromide (0.5 mmol, 1 equiv.) was heated and dissolved in absolute acetonitrile (3 mL). The ligand TMGasme (0.5 mmol, 1 equiv.) was added to the solution. The solution was filtered and red crystals were obtained by gas phase diffusion of diethyl ether in a yield of 0.076 g (0.163 mmol, 33%).

[$FeBr_2$(TMGasme)] (**1**) IR (KBr): $\tilde{\nu}$ = 2950 w (v($CH_{aliph.}$)), 1720 vw, 1637 vs (v(C=O)), 1570 s (v($C{=}N_{gua}$)), 1556 m (v($C{=}N_{gua}$)), 1516 s, 1477 m, 1443 m(v($C{=}C_{arom.}$)), 1420 m (v(C–H), 1409 m, 1396 vs, 1341 m, 1329 m, 1263 s(v(C-O-C_{ester})), 1247 s(v(C-O-C_{ester})), 1197 m, 1160 s, 1143 m, 1094 s, 1056 m, 1049 m, 1031 s, 965 m, 922 w, 871 m(v(C–$H_{arom.}$)), 846 w, 806 s, 756 vs, 715 w, 705 s, 666 m, 626 w, 578 w, 534 m, 517 m, 444 w, 428 w cm^{-1}; HR-MS ESI (+): m/z: calculated: 384.00101 [$C_{13}H_{19}{}^{79}BrFeN_3O_2$]$^+$ and 385.99896 [$C_{13}H_{19}{}^{81}BrFeN_3O_2$]$^+$; found: 384.00131 and 385.99905; EA $C_{13}H_{19}Br_2FeN_3O_2$ (465 g mol^{-1}) calculated: C 33.58, H 4.12, N 9.04 found: C 33.59, H 4.05, N 9.05.

Table S1. Crystallographic details of **1**.

Parameter	[FeBr$_2$(TMGasme)] **1**
empirical formula	$C_{13}H_{19}Br_2FeN_3O_2$
formula mass [g mol^{-1}]	262.98
crystal size [mm]	0.25 x 0.19 x 0.13
T [K]	100
crystal system	Monoclinic
space group	*P*2$_1$/n
a [Å]	11.439(2)
b [Å]	9.1071(18)
c [Å]	17.367(4)
α [°]	90
β [°]	103.01(3)
γ [°]	90
V [Å^3]	1762.9(6)
Z	4
ρ_{cal} [mg cm^{-3}]	1.752
μ [mm^{-1}]	5.395
λ [Å]	0.71073
F(000)	920
hkl range	-17≤ h ≤17, -7 ≤ k ≤13, -25 ≤ l ≤ 25
reflections collected	21478
Independen reflections	6110
R$_{int}$	0.0500
number of parameters	195
R$_1$ [*I*>2σ(*I*)]	0.0376
wR$_2$ (all data)	0.0722
goodness-of-fit	0.891
Largest diff. peak, hole [e$^-$ Å^{-3}]	0.664, -0.858

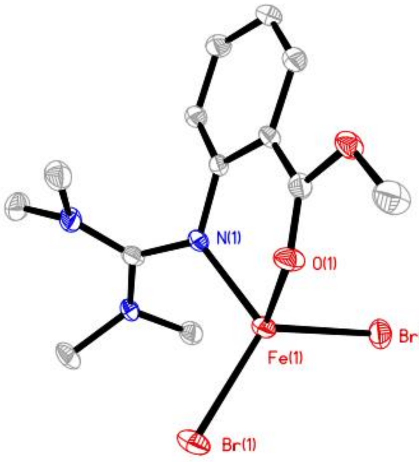

Figure S1. Molecular structures of **1** in the solid state (ellipsoids drawn at the 50% probability level). Hydrogen atoms are omitted for clarity.

The single crystal diffraction data for **1** are presented in Table S14. The data for **1** were collected with a four-circle goniometer Stoe Stadivari with Dectris Pilatus3 R 200 K hybrid pixel detector using Geni 3D high flux Mo-Ka radiation (λ = 0.71073 Å) at 100K. Temperature control was achieved with an Oxford Cryostream 800.

Crystals were mounted with grease on glass fibers. Data were collected with X-Area Pilatus and integrated with X-Area Integrate and X-Area Recipe. The absorption correction was performed by Gaussian integration with Stoe X-Red32, afterwards scaling of reflections with X-Area LANA.[3]

The structure was solved by direct and conventional Fourier methods and all non-hydrogen atoms were refined anisotropically with full-matrix least-squares based on F² (XPREP[65], SHELXS-97[66] and ShelXle[67]). Hydrogen atoms were derived from difference Fourier maps and placed at idealised positions, riding on their parent C atoms, with isotropic displacement parameters Uiso(H) = 1.2Ueq(C) and 1.5Ueq(C methyl). All methyl groups were allowed to rotate but not to tip.

Full crystallographic data have been deposited with the Cambridge Crystallographic Data Centre as supplementary no. CCDC – 2073861 for **1**. Copies of the data can be obtained free of charge on application to CCDC, 12 Union Road, Cambridge CB2 1EZ, UK (fax: (+44)1223-336-033; e-mail: deposit@ccdc.cam.ac.uk).

Table S2. Bond lengths and angles of **1** and the analogue chloride complex.

		1 [Fe**Br**$_2$(TMGasme)]	[Fe**Cl**$_2$(TMGasme)][4]
Bond lengths [Å]	Fe1-X1	2.393(1)	2.254(1)
	Fe1-X2	2.406(1)	2.239(1)
	Fe1-O1	2.042(2)	2.063(2)
	Fe1-N1	2.041(1)	2.048(2)
	C01-N1	1.350(1)	1.349(1)
	C01-N2	1.345(1)	1.341(1)
	C01-N3	1.347(1)	1.345(1)
Bond angles [°]	X1-Fe1-X2	122.1(1)	124.9(1)
	X1-Fe1-N1	114.3(1)	116.6(1)
	X2-Fe1-N1	113.9(1)	108.5(1)
	X1-Fe1-O1	109.3(1)	106.5(1)
	X2-Fe1-O1	103.7(1)	106.2(1)
	O1-Fe1-N1	86.4(1)	87.1(1)
	N1-C01-N2	122.5(1)	119.9(2)
	N1-C01-N3	118.9(1)	122.2(2)
	N2-C01-N3	118.5(1)	117.8(2)
Plane angles [°]	Fe1X1X2-Fe1O1N1	87.5(1)	87.6(1)
	Fe1O1N1-N1C01N2	42.8(1)	45.9(2)
	N3C4C5-N1N2N3	29.6(2)	32.0(2)
	C10C8C6-N1N2N3	65.3(1)	66.2(1)
τ_4 [ ][a]		0.88	0.84
ρ [ ][b]		1.00	1.00

[a] τ_4 = [360° - (α+β)] / 141°[5], [b] ρ = 2a / (b+c)[6].

Polymerization procedures

ROP monitored by reactRaman

In a nitrogen filled glove box, recrystallized *L*-lactide (8.0 g, 55.5 mmol, 1000 eq.) and crystalline **1** (7.74 mg, 0.0555 mmol, 1 eq.) were weighted in, mixed in a mortar, filled in a glass vial and removed from the glove box. The reactor was heated to the desired temperature under vacuum and flushed three times with argon. The reaction was conducted under argon atmosphere and sample collection started after the reaction mixture insertion as soon as the reactor was closed with a shaft drive stirrer with agitator speed control ("minisprint", *premix reactor AG*, Switzerland) and a stirring speed of 260 rpm was reached. The spectra were measured with a RXN1 spectrometer of Kaiser Optical Systems. The laser was used at a wavelength 785 nm and 450 mW through a probe head with sapphire lenses (d = 0.1 mm). The reaction time was adjusted to the monomer-to-initiator (M/I) ratio. The polymer was removed from the reactor and a ^{1}H NMR spectrum in $CDCl_3$ was collected to determine the conversion. The reaction mixture was dissolved in an appropriate amount of DCM, the polymer was precipitated in ethanol at room temperature, dried under vacuum and characterized via GPC. Kinetic data were obtained by integration of the Raman spectrum with the program *Peaxact 4* from *S-PACT GmbH*, boundaries were 627 – 674 cm^{-1} for lactide.

ATRP in Schlenk tubes

In a nitrogen filled glovebox crystalline **1** (139.5 mg, 0.3 mmol, 1 eq.) and the co-initiator BrPhOH (60.3 mg, 0.3 mmol, 1 eq.) was weighted into a Schlenk tube equipped with a stirring bar. The Schlenk tube was closed with a septum and removed from the glovebox. Under Schlenk technique, styrene (3.43 mL, 30 mmol, 100 eq.) was added to the reaction mixture with a gas-tight syringe. The Schlenk tube was placed in an aluminium block at 110 °C and stirred at 800 rpm. During the polymerization samples were removed under Schlenk technique with 1 mL syringes and collected in small glass vials. If the viscosity was too high for syringes, glass pipettes were used for sample removal by lifting the septum temporarily. A small amount of the sample was used to collect a ^{1}H NMR in $CDCl_3$ for conversion determination. The remaining polymer was dissolved in DCM and precipitated in ethanol. The suspension was centrifugated, the solvent was removed and fresh ethanol added to wash the polymer. After a second centrifugation the polymer was removed from the centrifugation vial, collected in a glass vial, dried under vacuum and characterized by GPC.

ATRP and ROP monitored by reactRaman

For a polymerization with a monomer to initiator to catalyst (M/I/Cat) ratio of 100+100:1:1 recrystallized and sublimed *L*-lactide (2882.6 mg, 20 mmol, 100 eq.), crystalline **1** (93.0 mg, 0.2 mmol, 1 eq.) and co-initiator BrPhOH (40.2 mg, 0.2 mmol, 1 eq.) were weighted in a nitrogen filled glovebox, mixed in a mortar, filled in a glass vial and removed from the glovebox. The reactor was heated to 110 °C under vacuum and flushed several times with argon. Degassed toluene (2 mL) was filled into the reactor under Schlenk technique with a gas-tight syringe and a baseline was recorded. Styrene (2.29 mL, 20 mmol, 100 eq.) was transferred to the reactor with a gas-tight syringe under Schlenk technique. Subsequently, the lactide/co-initiator/catalyst mixture was added to the reactor and sample collection was started as soon as the reactor was closed with a shaft drive stirrer with agitator speed control ("minisprint", *premix reactor AG*, Switzerland) and a stirring speed of 260 rpm was reached. The spectra were measured with a RXN1 spectrometer of Kaiser Optical Systems. The laser was used at a wavelength 785 nm and 450 mW through a probe head with sapphire lenses (d = 0.1 mm). The reaction time was adjusted to the monomers and M/I/Cat ratio. The reaction mixture was removed from the reactor and a ^{1}H NMR spectrum in $CDCl_3$ was collected to determine the conversion. The reaction mixture was dissolved in an appropriate amount of DCM, the polymer was precipitated in ethanol at room temperature, dried under vacuum and characterized *via* GPC. Kinetic data were obtained by integration of the Raman spectrum with the program *Peaxact 4* from *S-PACT GmbH*, boundaries were 627 – 680 cm^{-1} for lactide and 1615 – 1660 cm^{-1} for styrene.

Results and Discussion

Lactide was polymerized by **1** and the polymerization activity was compared with the chloride analogue.[4] The semilogarithmic plot is shown in Figure S2.

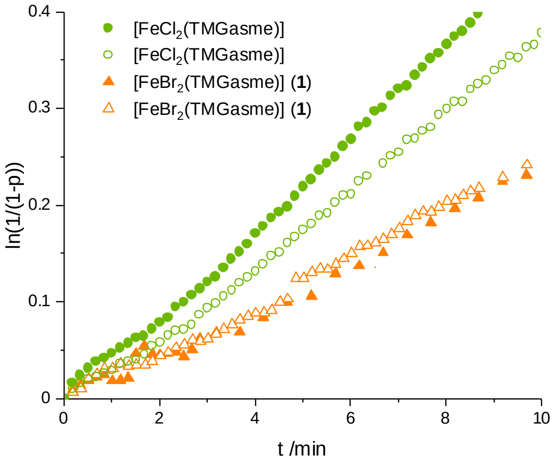

Figure S2. Semilogarithmic plot of the polymerization of lactide with **1** and its chloride analogue. M/I ratio 1000:1, bulk polymerization at 150 °C and 260 rpm.

The relative conversion for kinetic plots was obtained by integration of the referring Raman band, the absolute conversion was calculated from the ^{1}H NMR spectra of the crude polymerization product as shown in Figure S3.

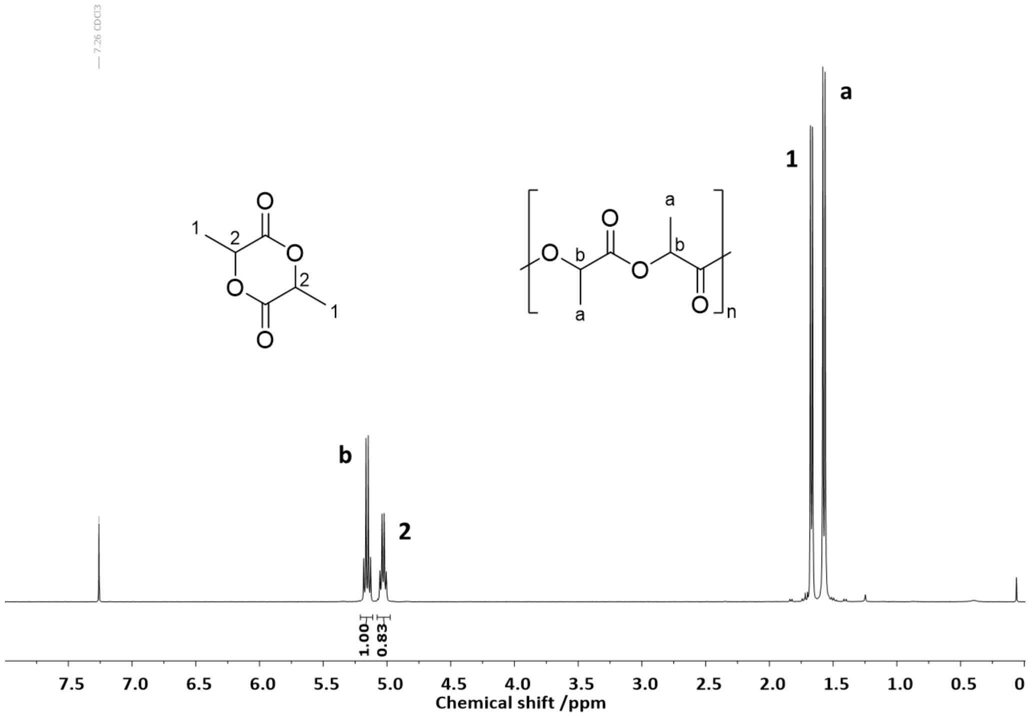

Figure S3. Exemplary ^{1}H NMR spectrum (400 MHz, $CDCl_3$) of a crude polymerization product of lactide to PLA. Conversion is calculated by

$$p(\text{LA}) = \frac{\int b}{\int b + \int 2} = \frac{1.00}{1.00+0.83} = 0.55.$$

1 was tested as catalyst in the polymerization of styrene. The data of the polymerizations are summarized in Table S3.

Table S3. Duplicate measurement of the polymerization of styrene.

Time[a]	10 min	20 min	30 min	40 min	50 min	1 h	1.5 h	2 h	2.5 h	3 h	3.5 h	4 h
Conversion p[b]	0.03	0.09	0.14	0.19	0.23	0.25	0.29	0.33	0.37	0.40	0.44	0.45
Error	0.01	0.00	0.01	0.01	0.01	0.01	0.01	0.00	0.00	0.00	0.02	0.01
ln(1/(1-p))	0.03	0.09	0.15	0.20	0.25	0.28	0.34	0.40	0.46	0.51	0.57	0.59
Error	0.01	0.00	0.01	0.01	0.01	0.01	0.01	0.00	0.00	0.00	0.03	0.01
$M_{n,theo}$[c]	-	-	-	4200	4600	5300	5500	6000	6200	6600	6800	6800
M_n[d]	-	-	-	3700	3600	3700	4700	5500	6200	6800	7100	7200
$Đ$[d]	-	-	-	1.15	1.09	1.09	1.09	1.10	1.12	1.12	1.14	1.16

[a] M/I/Cat ratio of 100:1:1, 110°C, 800 rpm, solvent-free. [b] Calculated from ^{1}H NMR spectrum. [c] Calculated by $M_{\mathrm{n,theo}} = p(\mathrm{styrene}) \cdot 104.15\ \mathrm{g\ mol^{-1}} \cdot 100$. [d] Obtained from GPC measurement.

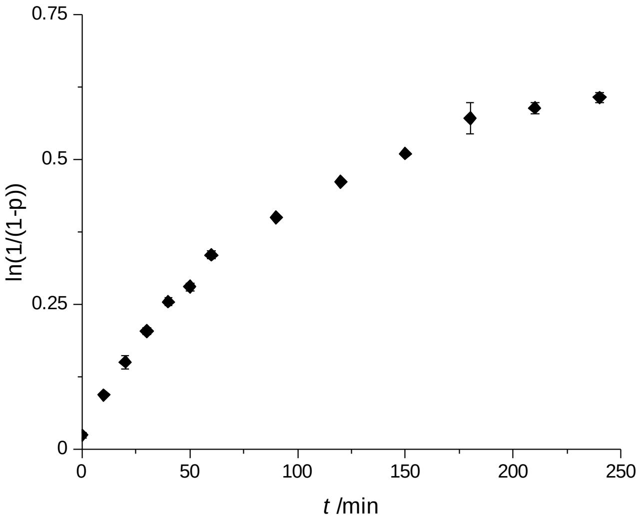

Figure S4. Semilogarithmic plot displaying full polymerization time of ATRP of styrene with a M/I/Cat ratio of 100:1:1 at 110 °C and solvent-free condition.

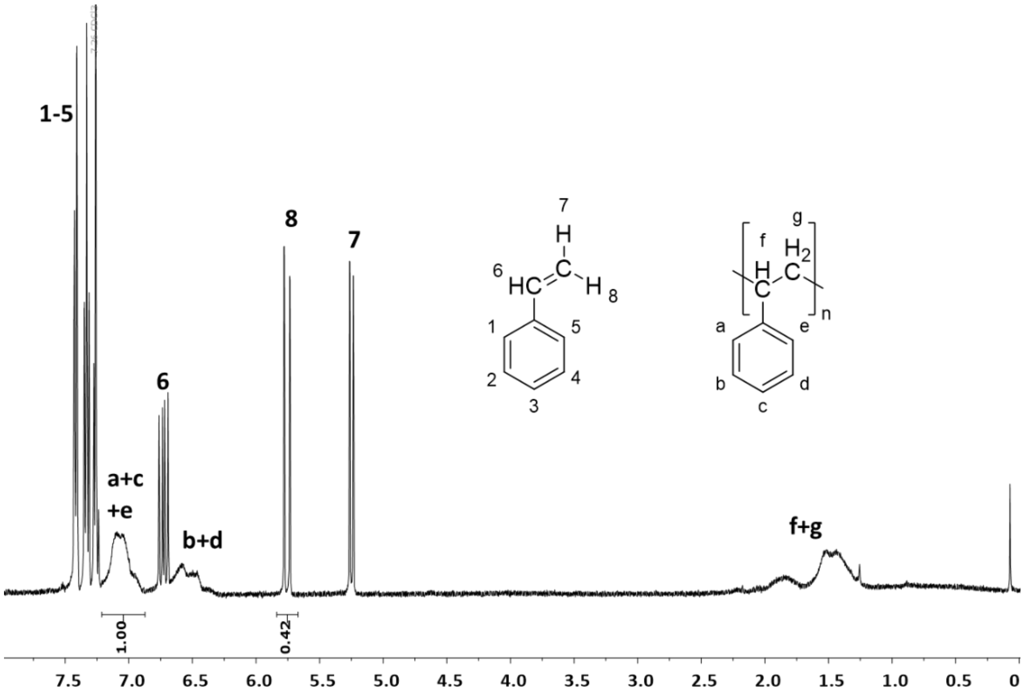

Figure S5. Exemplary ^{1}H NMR spectrum (400 MHz, CDCl$_3$) of a crude polymerization product of styrene to PS. Conversion is calculated by

$$p(\mathrm{S}) = \frac{(\int a+c+e)/3}{(\int a+c+e)/3+\int 8} = \frac{1.00/3}{1.00/3+0.42} = 0.44.$$

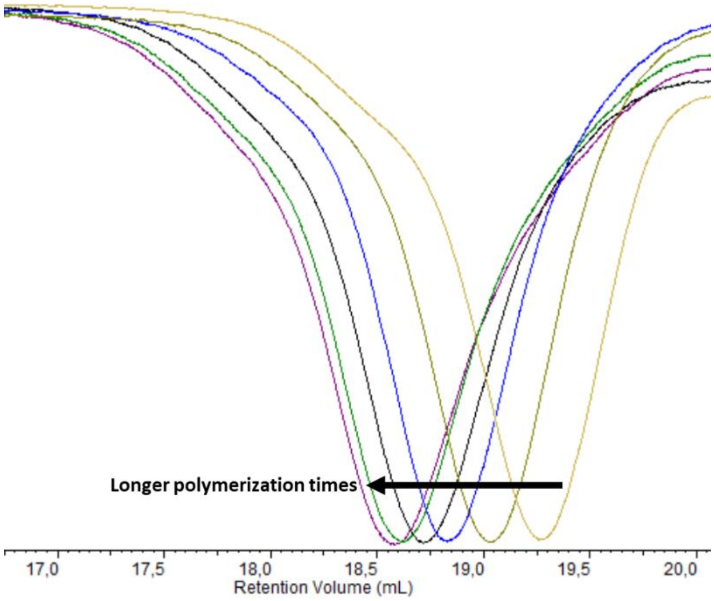

Figure S6. GPC traces of ATRP of styrene with a M/I/Cat ratio of 100:1:1, 110°C under solvent-free conditions at different polymerization times.

Table S4 contains information on ATRP with a reaction mixture missing one or several components.

Table S4. ATRP with different components.

Components added[a]	Time	Conversion[b]	$M_{n,theo}$[c] /(g mol^{-1})	M_n[d] /(g mol^{-1})	M_w[d] /(g mol^{-1})	$Đ$[d]
$FeBr_2$, TMGasme, BrPhOH[e]	3 h	0.47	7700	7600	12300	1.5
$FeBr_2$, BrPhOH	0.5 h	0.99	10300	4700	8200	1.7
TMGasme, BrPhOH	3 h	0.09	2400	39800	96000	2.4
BrPhOH	3 h	0.03	830	120000	187000	1.6

[a] In addition to 100 eq. of styrene. 1 eq. of each component. [b] Calculated from ^{1}H NMR spectrum. [c] Calculated by $M_{\mathrm{n,theo}} = p(\mathrm{styrene}) \cdot 104.15\ \mathrm{g\ mol^{-1}} \cdot 100$. [d] Obtained from GPC measurement. [e] $FeBr_2$ and TMGasme were added separately for the catalyst to form *in situ*.

Lactide and styrene were polymerized simultaneously. Figure S7 – S13 give details on the polymerization and the produced polymer.

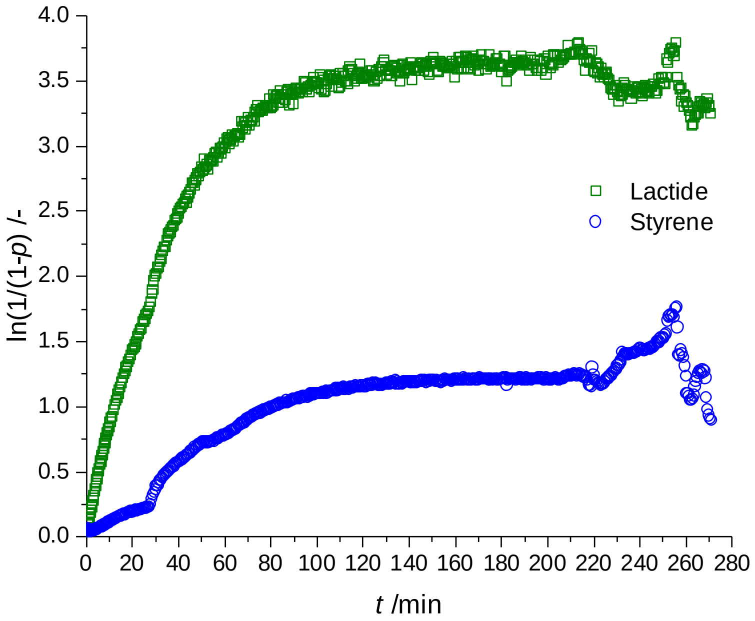

Figure S7. Semilogarithmic plot of orthogonal copolymerization of styrene and lactide (run 1, Table 2) (full polymerization time).

The polymers produced by simultaneous or sequential copolymerization (see Table 2) were analyzed by NMR.

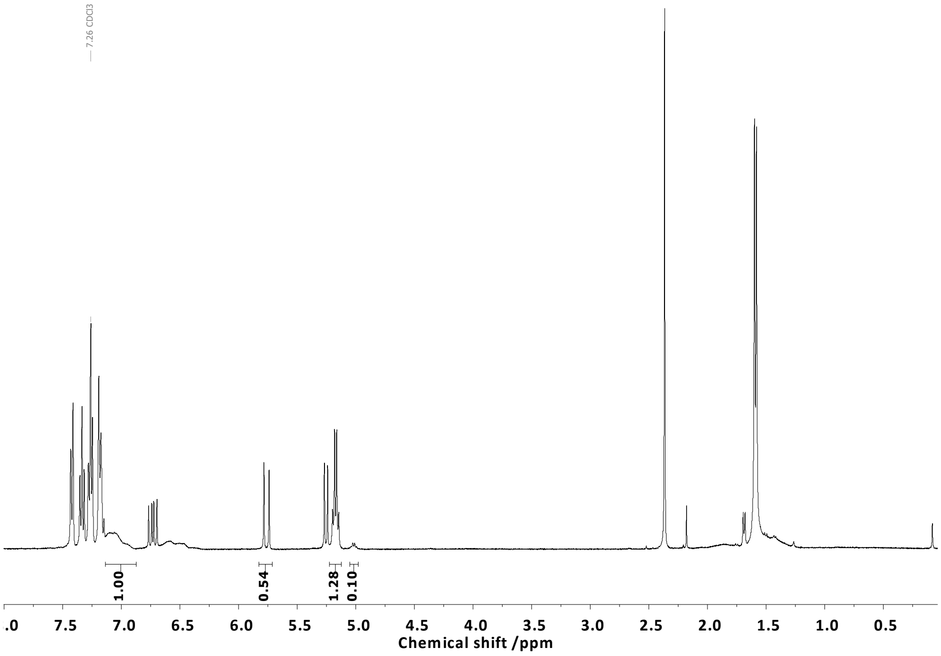

Figure S8. ^{1}H NMR spectrum (400 MHz, $CDCl_3$) of the crude polymerization product of the orthogonal copolymerization of lactide and styrene with integrated peaks for conversion determination (run 1, Table 2).

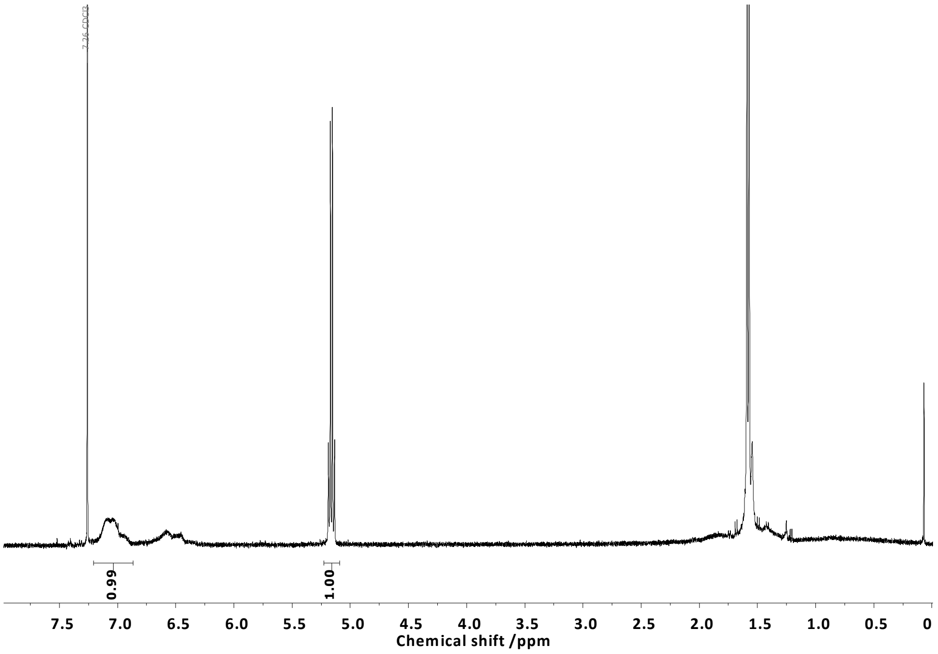

Figure S9. ^{1}H NMR spectrum (400 MHz, $CDCl_3$) of the precipitated polymerization product of the orthogonal copolymerization of lactide and styrene (run 1, Table 2). The incorporation ratio was calculated by the ratio of the referring polymeric signals normalized to the number of hydrogen atoms they represent (see Figure S5). Here: 0.99/3 : 1.00 = 0.33 : 1.00.

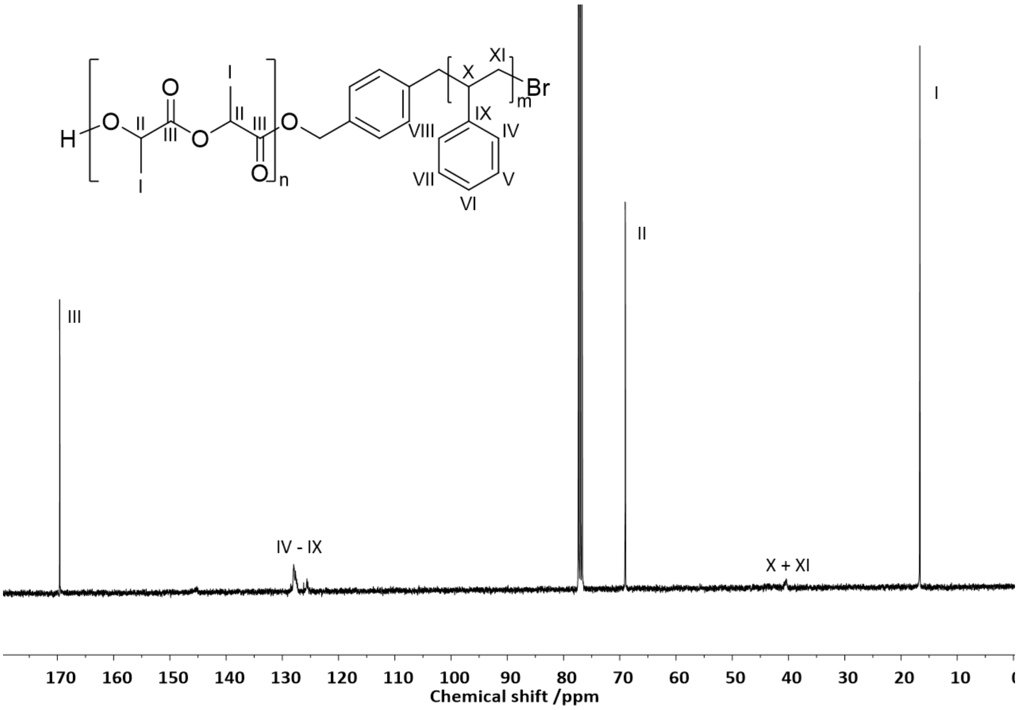

Figure S10. ^{13}C NMR spectra (101 MHz, $CDCl_3$) of the precipitated polymerization product of the orthogonal copolymerization of lactide and styrene (run 1, Table 2). The PLA signal of the carbonyl group is represented by a single peak at 170.0 ppm.

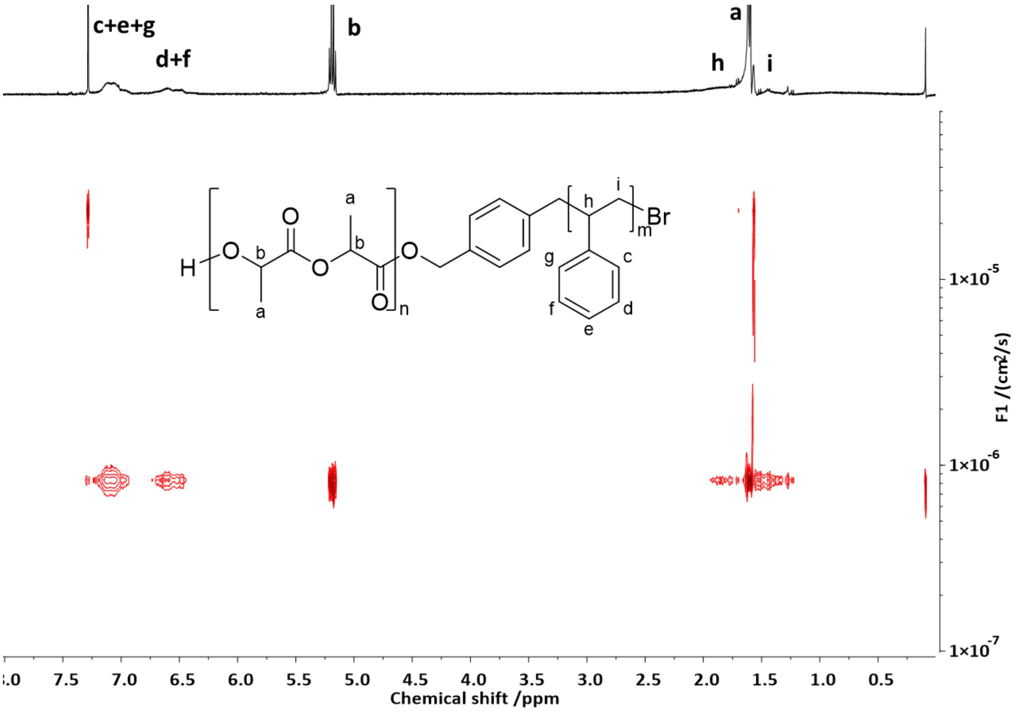

Figure S11. DOSY data (400 MHz, $CDCl_3$) of the precipitated product of the orthogonal copolymerization of lactide and styrene (run 1, Table 2).

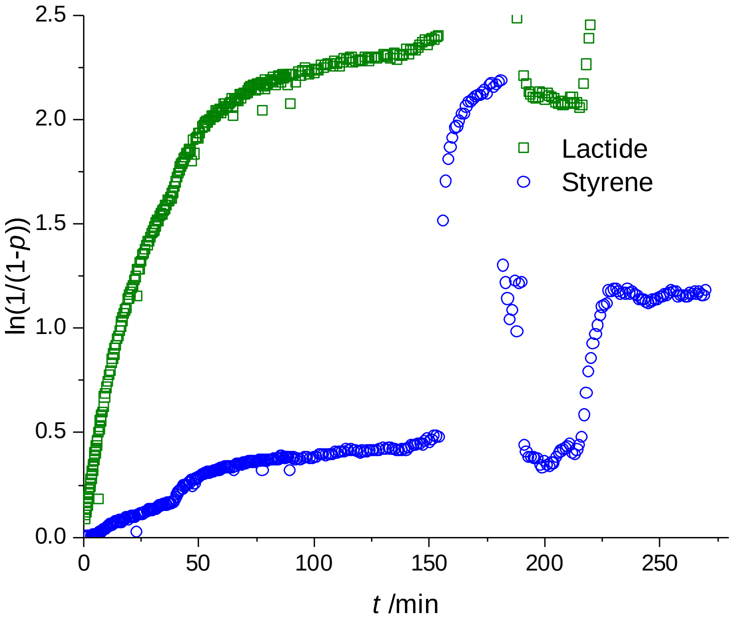

Figure S12. Semilogarithmic plot of orthogonal copolymerization of lactide and styrene (run 2, Table2). Data above a reaction time of 150 min show strong spectroscopic fluctuations.

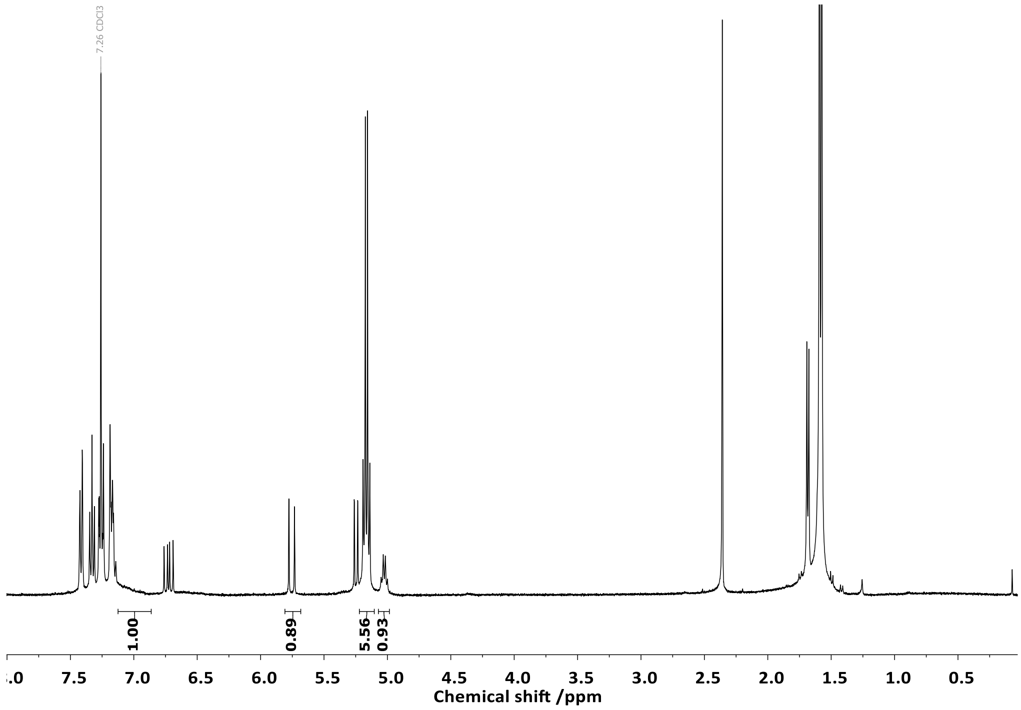

Figure S13. ^{1}H NMR spectrum (400 MHz, $CDCl_3$) of the crude polymerization product of the orthogonal copolymerization of lactide and styrene with integrated peaks for conversion determination (run 2, Table 2).

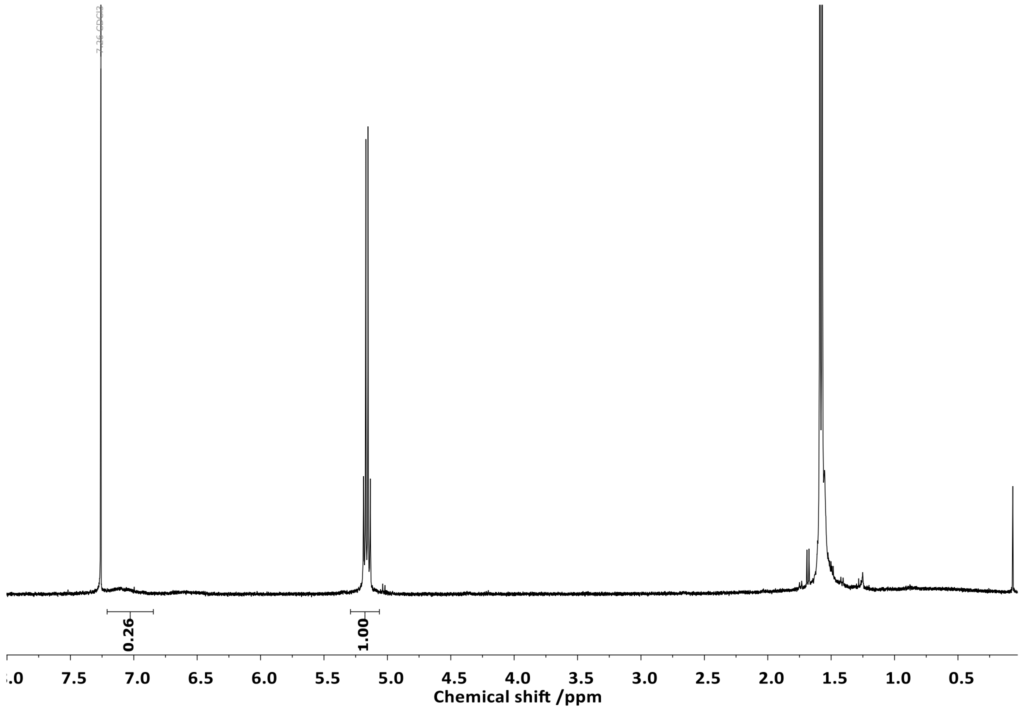

Figure S14. ^{1}H NMR spectrum (400 MHz, $CDCl_3$) of the precipitated polymerization product of the orthogonal copolymerization of lactide and styrene with integrated peaks for incorporation ratio determination (run 2, Table 2).

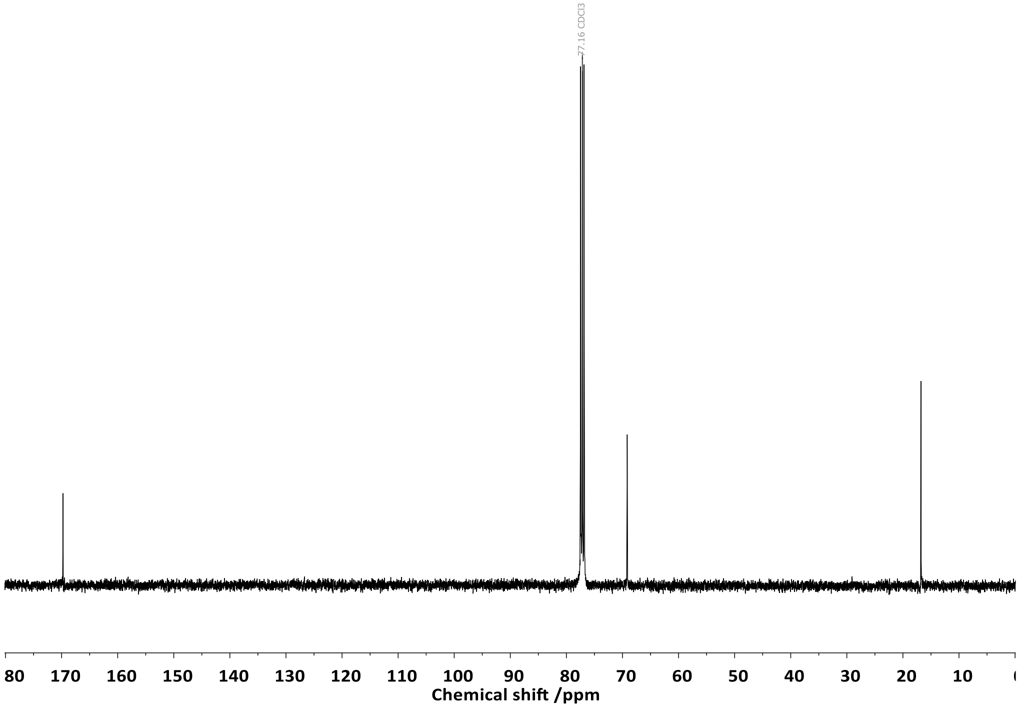

Figure S15. ^{13}C NMR spectra (101 MHz, $CDCl_3$) of the precipitated polymerization product of the orthogonal copolymerization of lactide and styrene (run 2, Table 2).

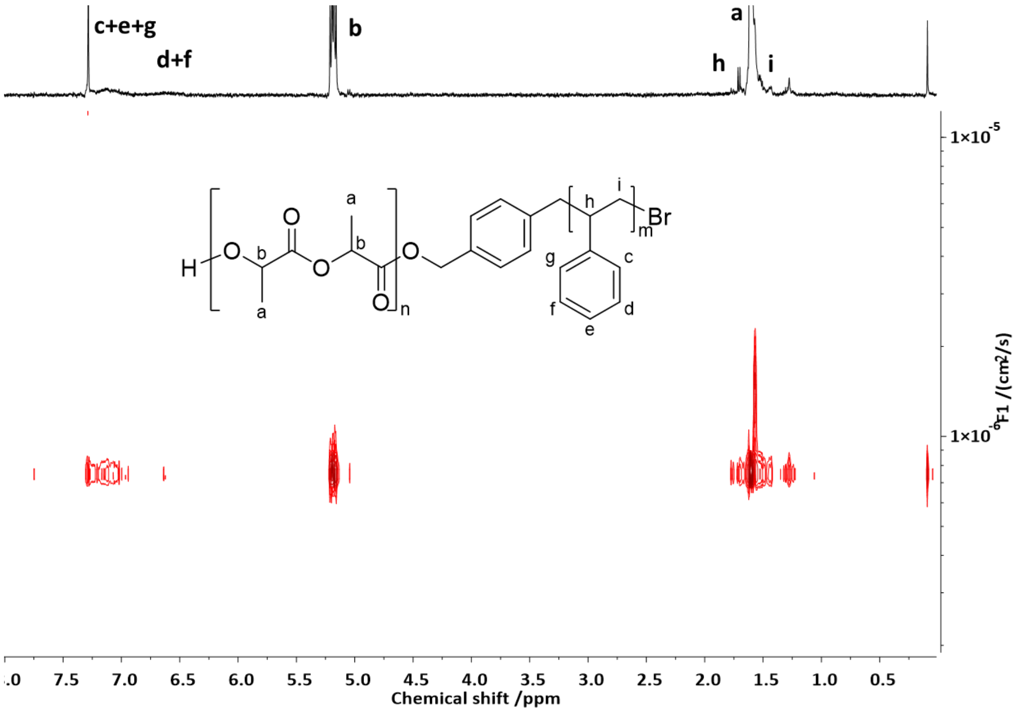

Figure S16. DOSY data (400 MHz, $CDCl_3$) of the precipitated product of the orthogonal copolymerization of lactide and styrene (run 2, Table 2).

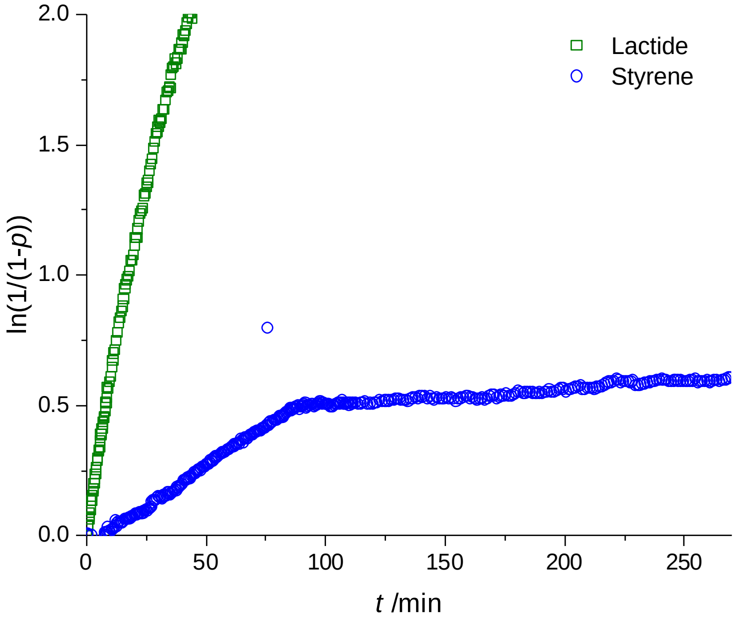

Figure S17. Semilogarithmic plot of orthogonal copolymerization of lactide and styrene (run 3, Table2).

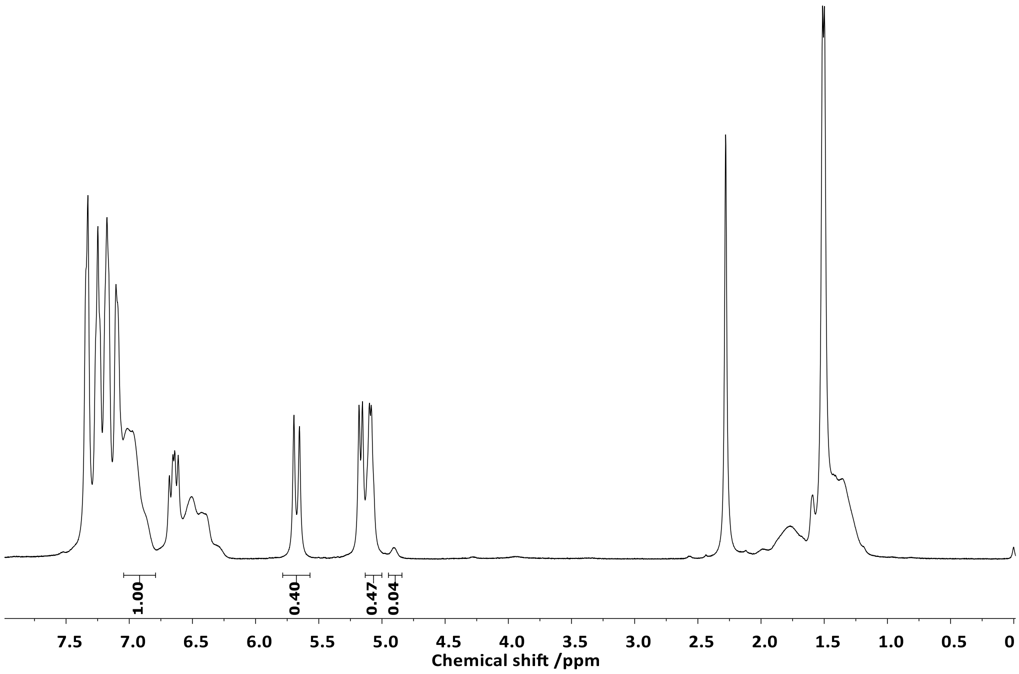

igure S18. ^{1}H NMR spectrum (400 MHz, $CDCl_3$) of the crude polymerization product of the orthogonal copolymerization of lactide and styrene with integrated peaks for conversion determination (run 3, Table 2).

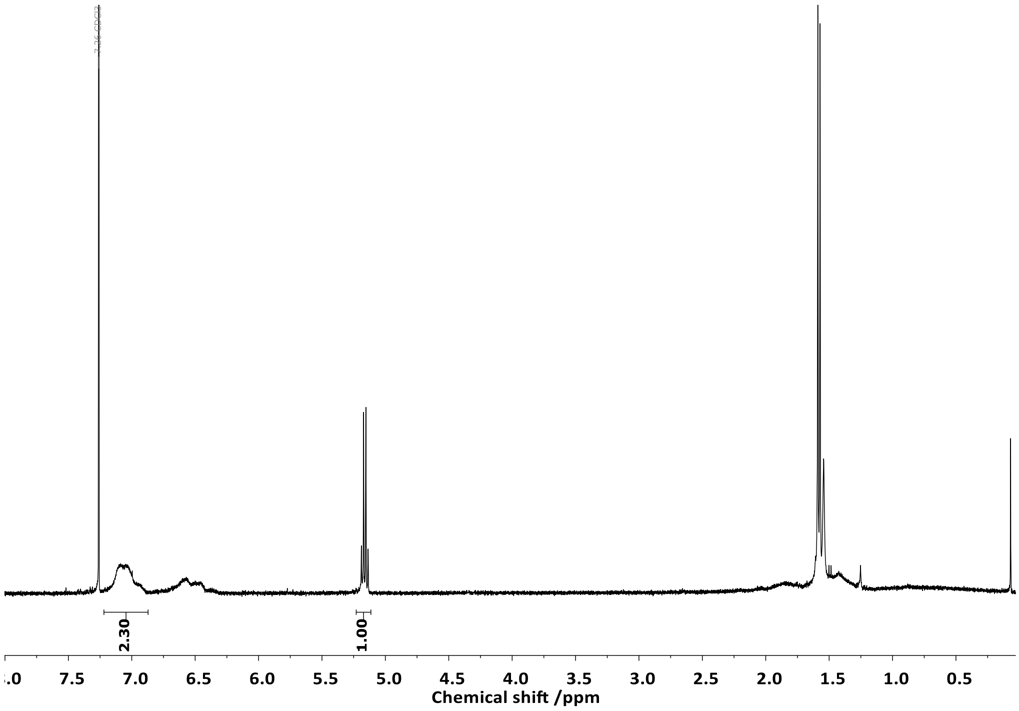

Figure S19. ^{1}H NMR spectrum (400 MHz, $CDCl_3$) of the precipitated polymerization product of the orthogonal copolymerization of lactide and styrene with integrated peaks for incorporation ratio determination (run 3, Table 2).

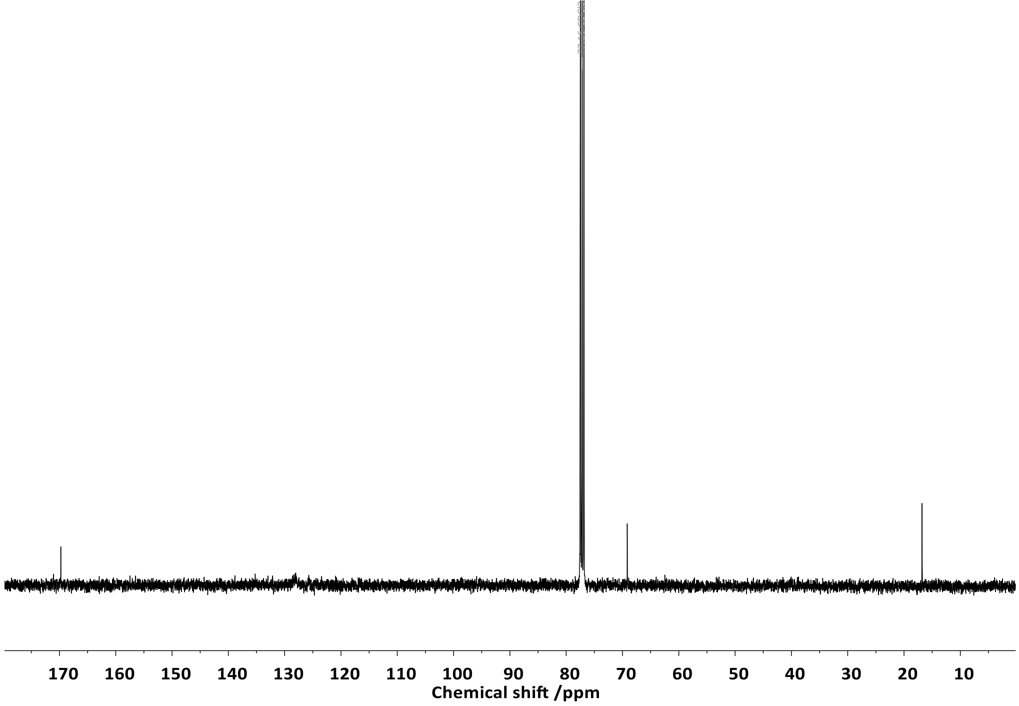

Figure S20. ^{13}C NMR spectra (101 MHz, $CDCl_3$) of the precipitated polymerization product of the orthogonal copolymerization of lactide and styrene (run 3, Table 2).

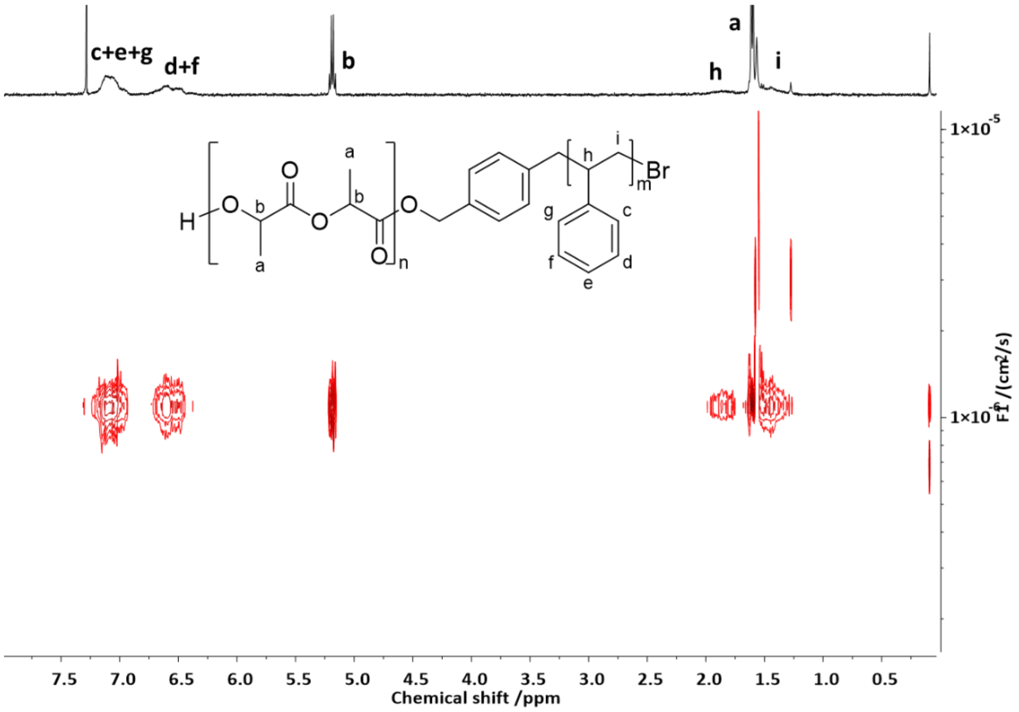

Figure S21. DOSY data (400 MHz, $CDCl_3$) of the precipitated product of the orthogonal copolymerization of lactide and styrene (run 3, Table 2).

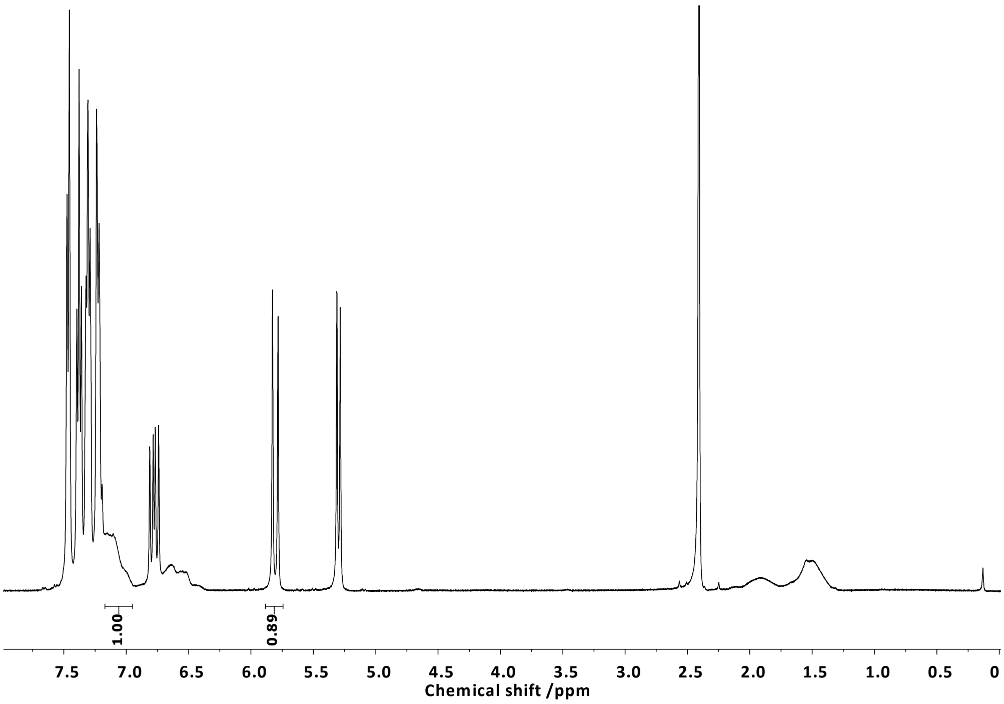

Figure S22. ^{1}H NMR spectrum (400 MHz, $CDCl_3$) of the crude polymerization product after 3 h of reaction time (before addition of lactide) integrated peaks for conversion determination (run 4, Table 2).

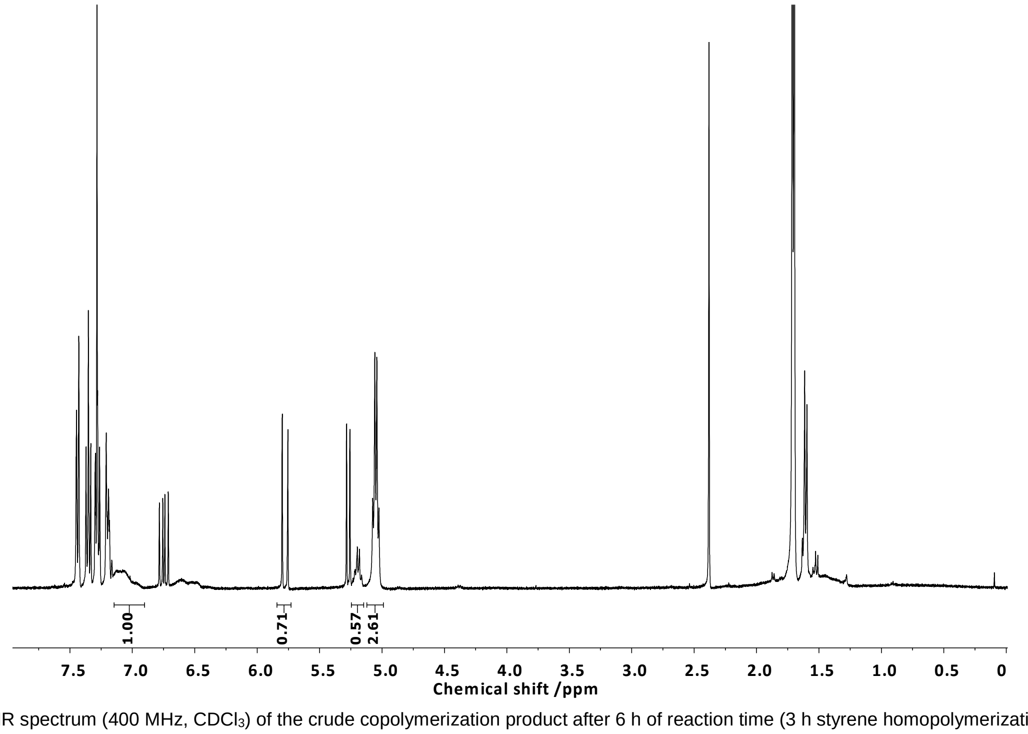

Figure S23. ^{1}H NMR spectrum (400 MHz, $CDCl_3$) of the crude copolymerization product after 6 h of reaction time (3 h styrene homopolymerization + 3 h lactide copolymerization) integrated peaks for conversion determination (run 4, Table 2).

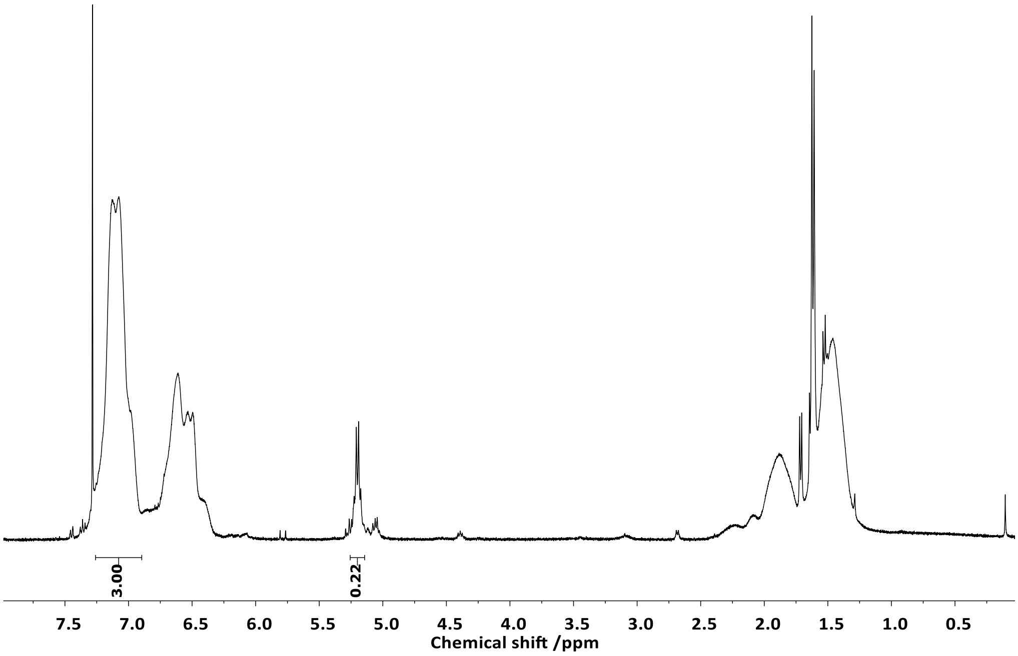

Figure S24. ^{1}H NMR spectrum (400 MHz, $CDCl_3$) of the precipitated copolymerization product of the sequential polymerization of lactide and styrene after 6 h with integrated peaks for incorporation ratio determination (run 4, Table 2).

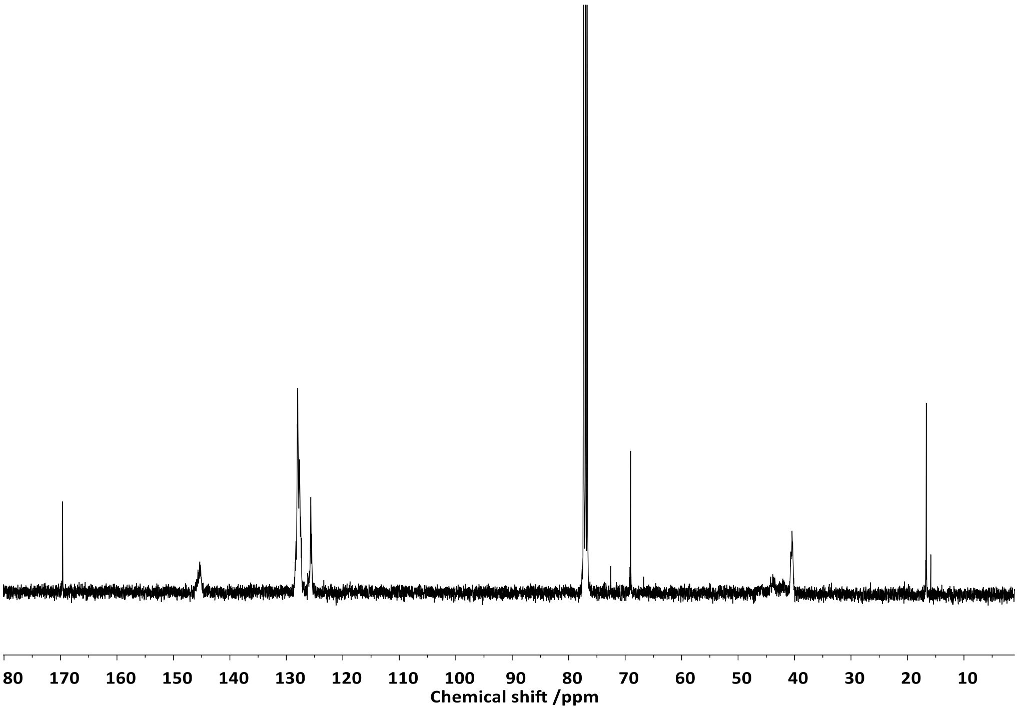

Figure S25. ^{13}C NMR spectrum (101 MHz, $CDCl_3$) of the precipitated copolymerization product of the sequential polymerization of lactide and styrene after 6 h (run 4, Table 2).

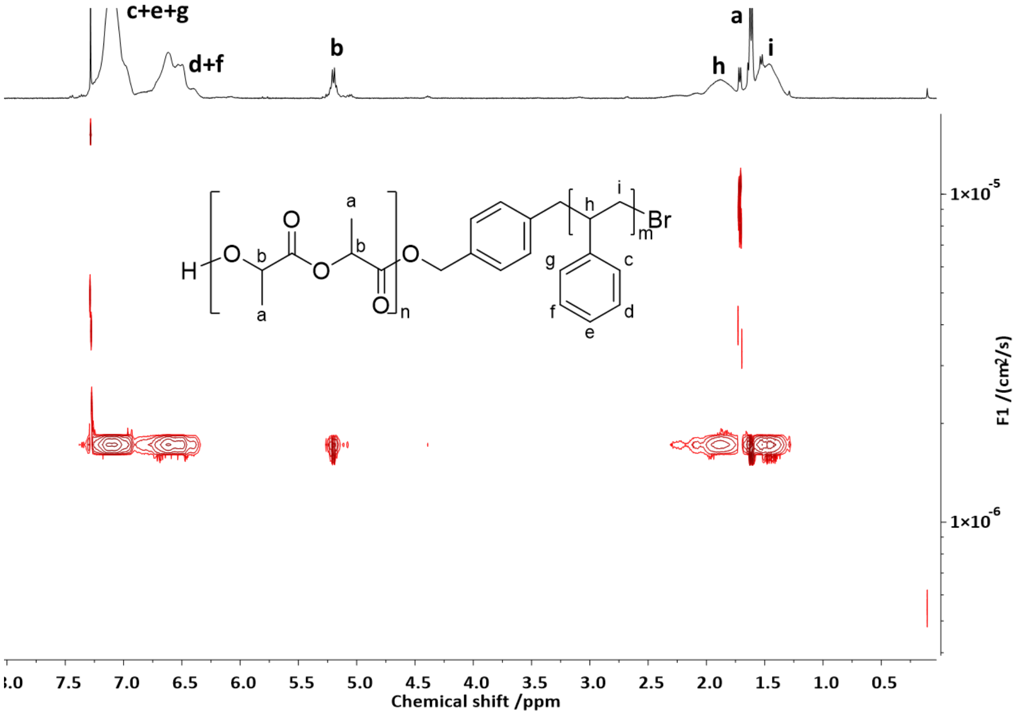

Figure S26. DOSY data (400 MHz, $CDCl_3$) of the precipitated product of the sequential polymerization of lactide and styrene (run4, Table 2).

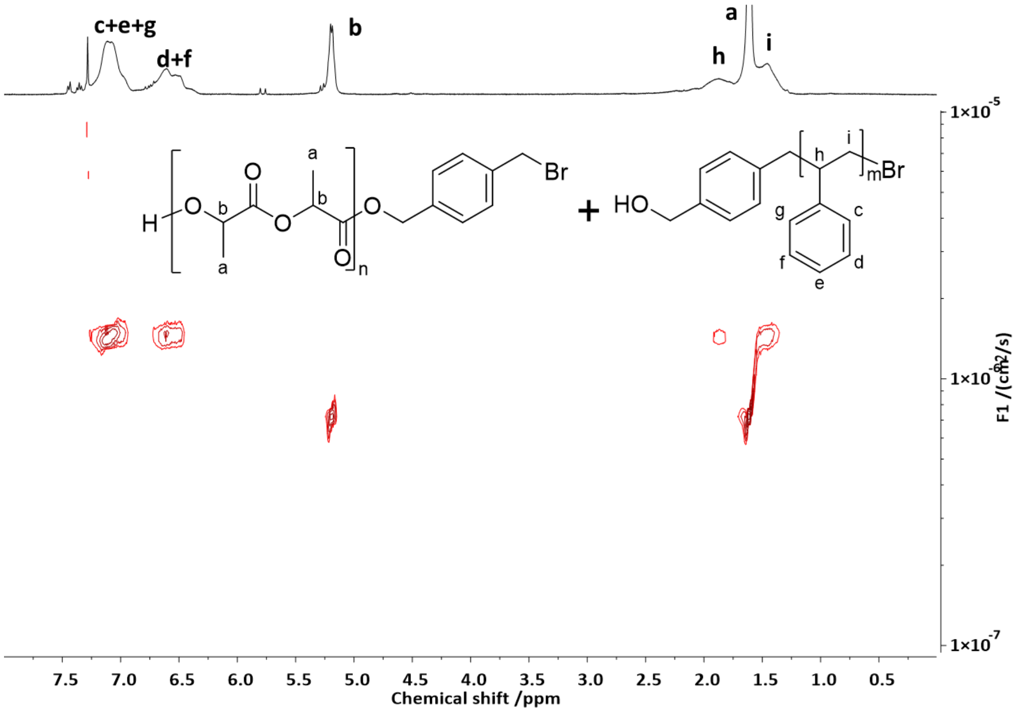

Figure S27. DOSY data (400 MHz, $CDCl_3$) of a mixture of PLA and PS homopolymers. Two different diffusion coefficients are visible.

The polymers were investigated with ^{1}H NMR spectroscopy to verify their connection to the bifunctional co-initiator. The spectra are displayed in Figure S28. The signals of the CH_2 groups of the co-initiator next to the initiating groups are visible in the polymer spectra and move when polymer is attached to the respective initiating group. The signal on the hydroxy side only moves slightly when PLA is attached (1a). Additionally, the signal broadens due to the polymeric surrounding. The signal on the bromide side is shifted drastically to the high field when PS is attached (2a) since the chemical surrounding changes from an electron withdrawing bromide atom to an aliphatic carbon atom. Due to the other signals in the aliphatic region, the corresponding signal could unfortunately not be localized. The signals of PS are very broad due to coiling of the polymer chain in $CDCl_3$. When lactide is homopolymerized to PLA with the bifunctional co-initiator, the signal of the bromide side (2) is maintained while the signal of the hydroxy side (1a) is shifted and broadened indicating the attachment of a polymer. When styrene is homopolymerized to PS in the presence of the bifunctional co-initiator the signal of the bromide side disappears (2) and probably reappears in the aliphatic region where it could not be detected (2a). Despite the maintenance of the hydroxy group on the other side of the co-initiator, the signal (1b) is shifting slightly and broadened due to the attachment to PS which is coiling intensively caused by poor solubility in chloroform. When the bifunctional co-initiator is used in the copolymerization of lactide and styrene, both initial signals (1 and 2) can no longer be found. Instead 1a appears corresponding to the attachment of PLA on the hydroxy side of the co-initiator. 2a is again not localized due to the more intensive signals in the aliphatic regions, however, its absence indicates the change in the chemical surrounding resulting from the connected PS initiated by the abstraction of the bromide atom. The presence or absence of the referring peaks hence confirm that both polymerization mechanisms are initiated by the bifunctional co-initiator.

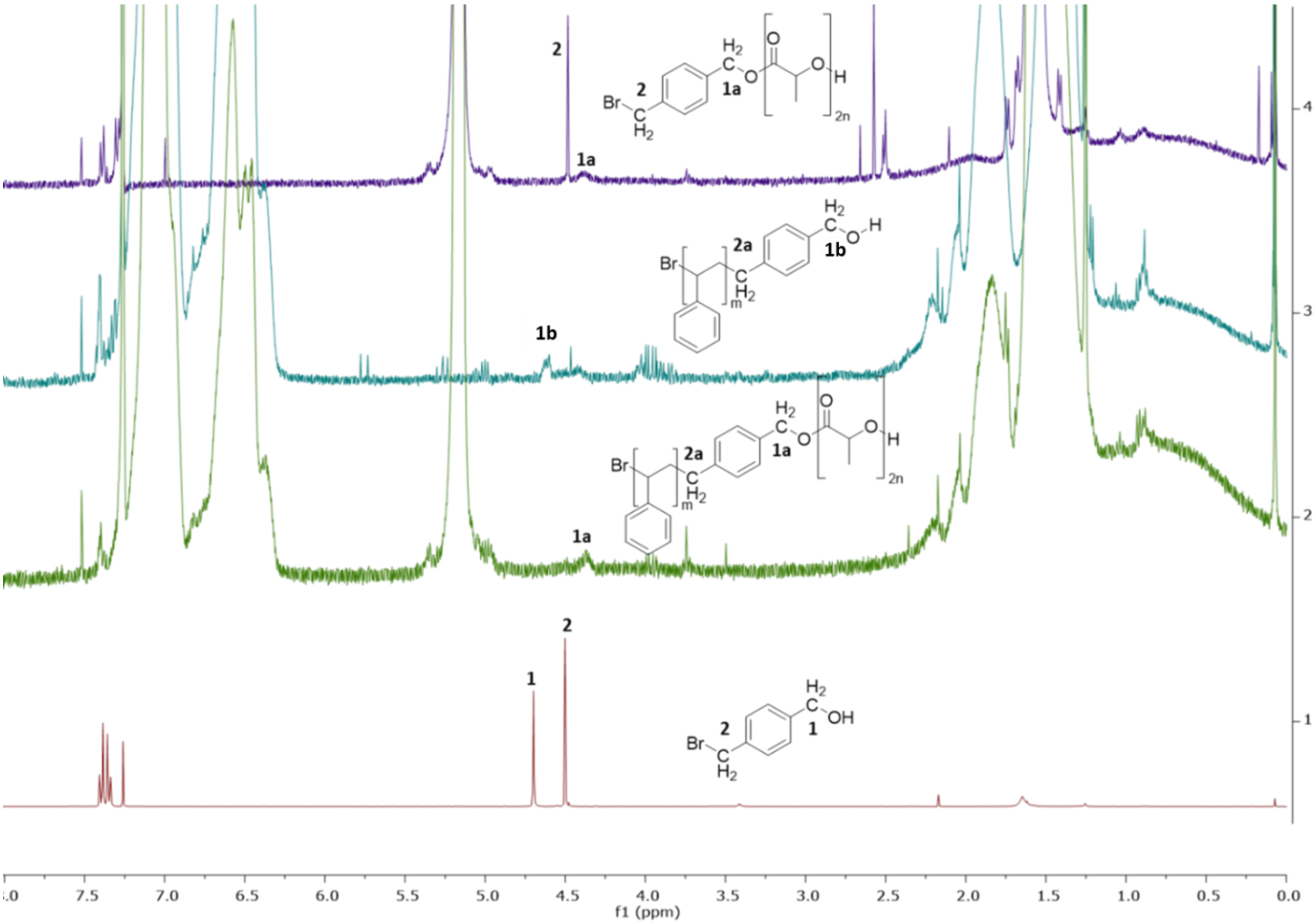

Figure S28. ^{1}H NMR spectra (400 MHz, $CDCl_3$) of different polymer species and the co-initiator.

To identify the active species for ROP in the simultaneous copolymerization, lactide was homopolymerized with the Fe^{II} complex **1** and the *in situ* generated Fe^{III} complex by mixing $FeBr_3$ and the ligand TMGasme. The graph in Figure S7 reveals a much higher polymerization activity of the Fe^{II} complex in comparison with the Fe^{III} complex.

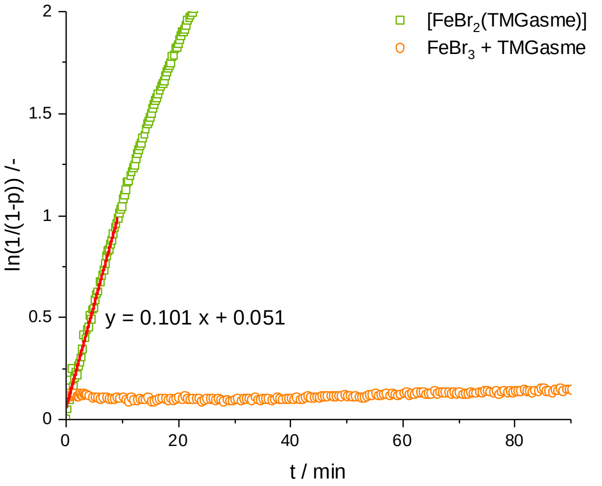

Figure S29. Semilogarithmic plot of the polymerization of lactide with the Fe^{II} complex **1** and the *in situ* generated Fe^{III} complex. Polymerization conditions: M/I/Cat ratio 100:1:1 (lactide:BrPhOH:catalyst), in 6.43 mL toluene, 110 °C and 260 rpm. Specification of the resulting PLA polymer: 95% conversion after 60 min, $M_{n,theo}$ = 23600 g mol^{-1}, M_n = 26900 g mol^{-1}, $Đ$ = 1.20.

The produced polymer was analyzed with GPC and a monomodal distribution was found indicating the formation of a block copolymer. Figure S5 shows refractive index signal of the GPC measurement.

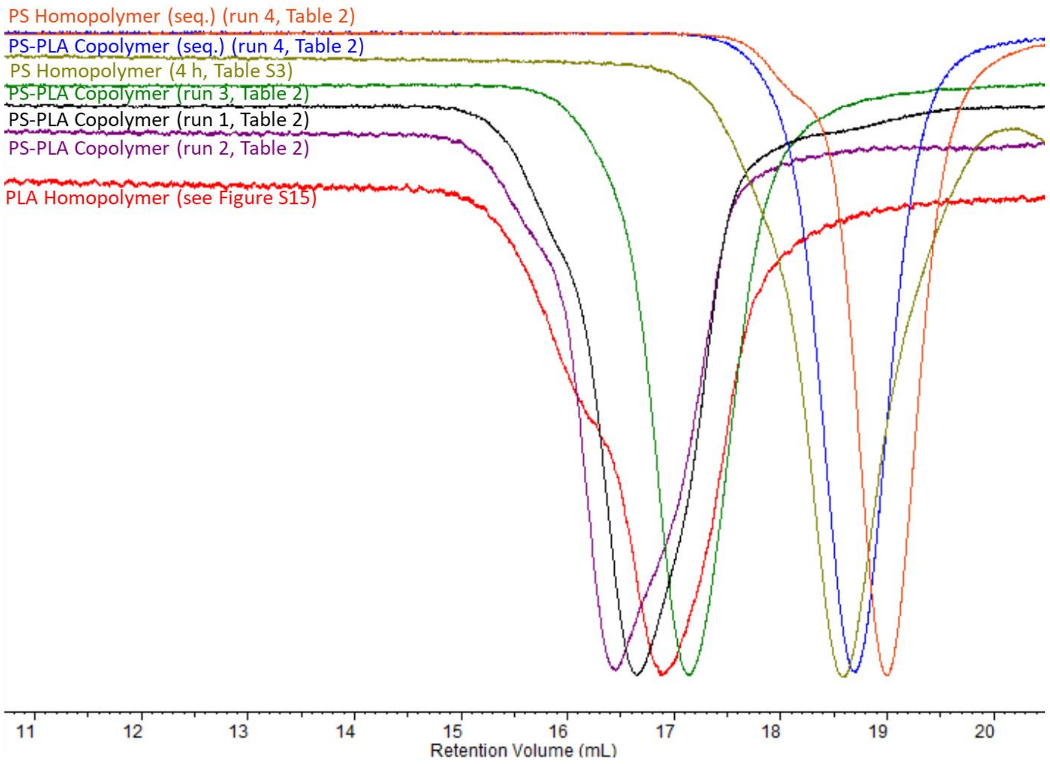

Figure S30. Refractive index signal of the GPC measurements of homo- and copolymers described in Table 2.

The produced homopolymers, the copolymers and a mixture of the homopolymers were analyzed with DSC. Table S6 summarizes the thermal parameters found and Figure S31-S36 displays the recorded thermograms.

Table S5. Thermal parameters obtained by DSC.

Sample	T_g /°C[a]	T_m /°C[a]	ΔH_m /Jg^{-1}[a]	X_c /%[b]
PLA homopolymer (see Figure S29)	n.m.	174	57	61
PS homopolymer (4 h, Table S3)	79	n.m.	n.m.	n.d.
Mixture of PLA and PS homopolymer (50 wt%)	98	173	26	28
PS-PLA copolymer (run 1, Table 2)	61	171	35	38
PS-PLA copolymer (run 2, Table 2)	60	173	56	60
PS-PLA copolymer (run 3, Table 2)	58	160[c]	32	56

[a] Values of second heating, n.m.: not measured, n.d.: not determined. [b] $X_c = \Delta H_m / \Delta H_m^0 \cdot 100$ with ΔH_m^0(PLA) = 93 Jg^{-1}[7]. [c] Melting peak of first heating.

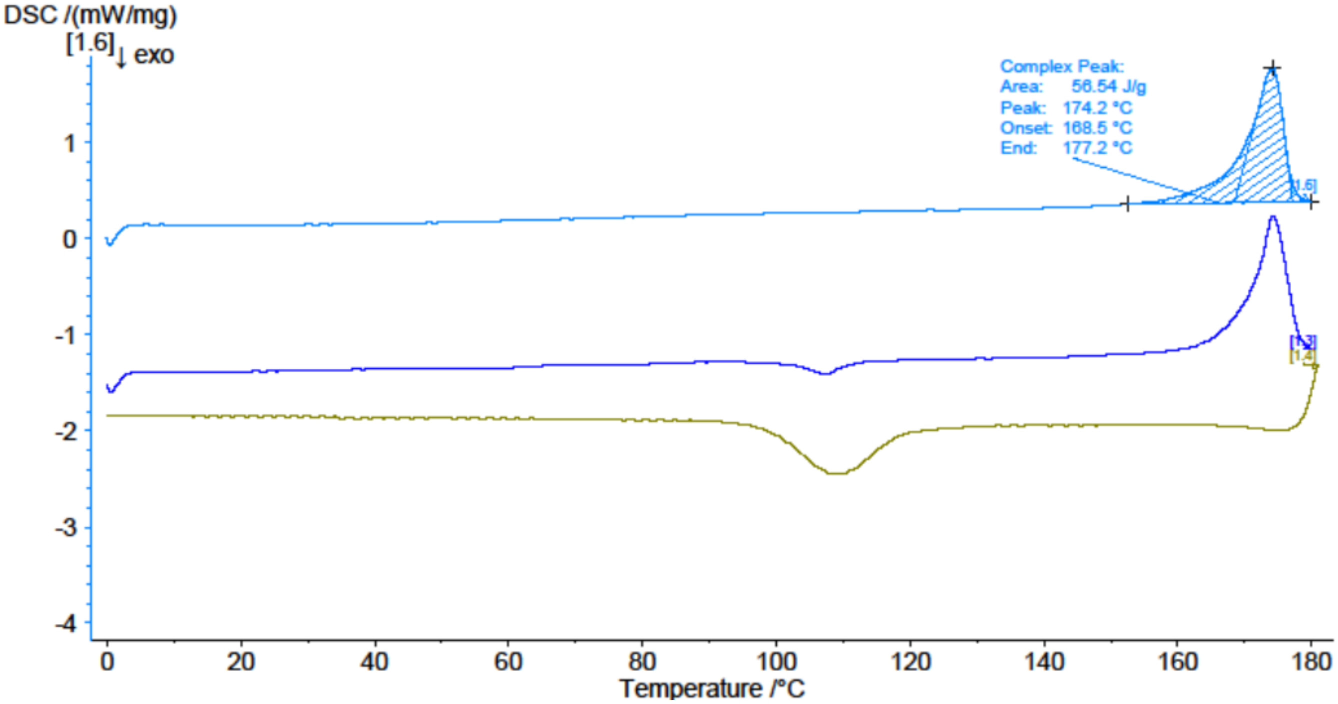

Figure S31. DSC thermogram of PLA homopolymer (see Figure S29).

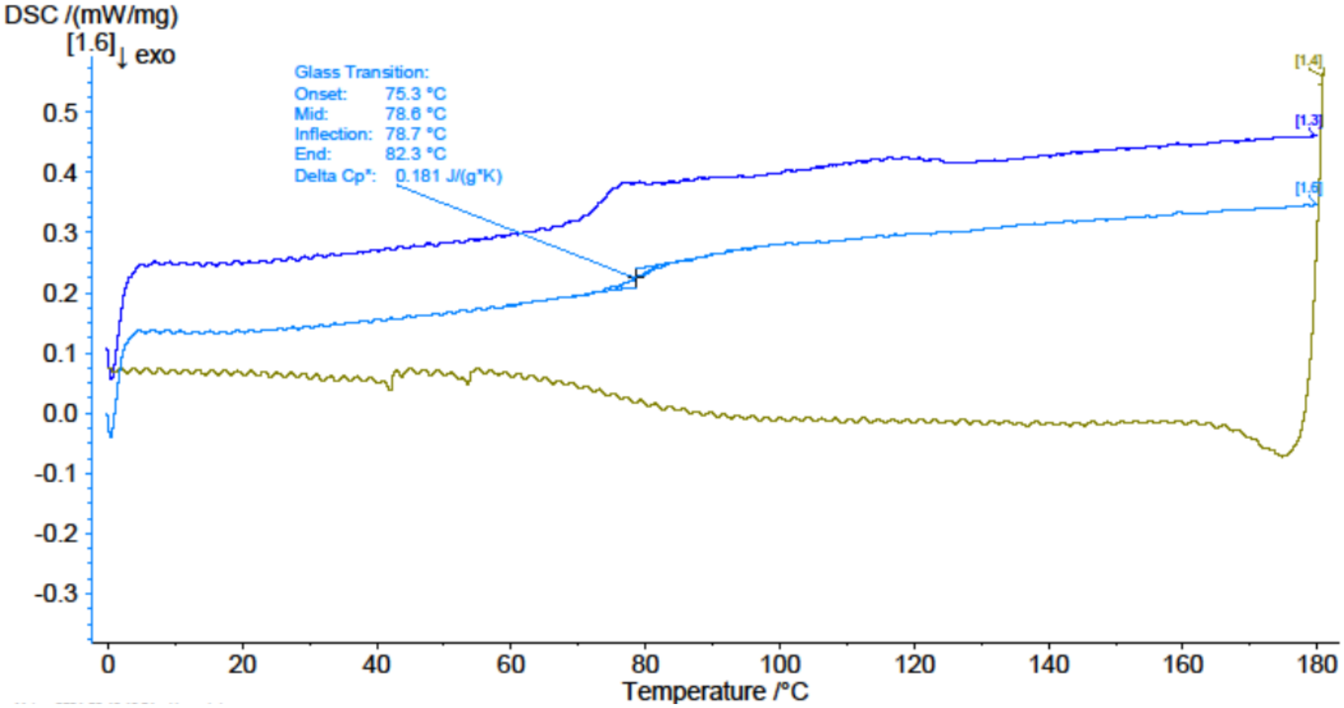

Figure S32. DSC thermogram of PS homopolymer (4 h, Table S3).

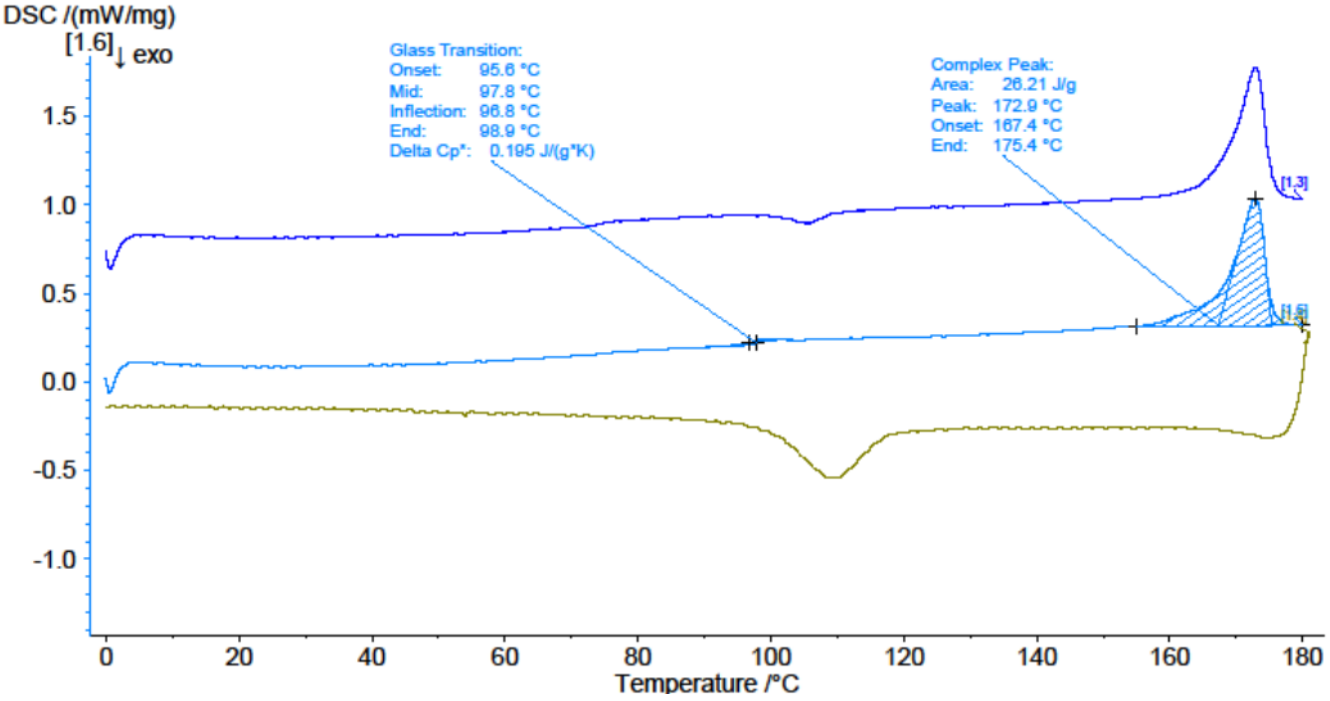

Figure S33. DSC thermogram of a mixture of PS and PLA homopolymer.

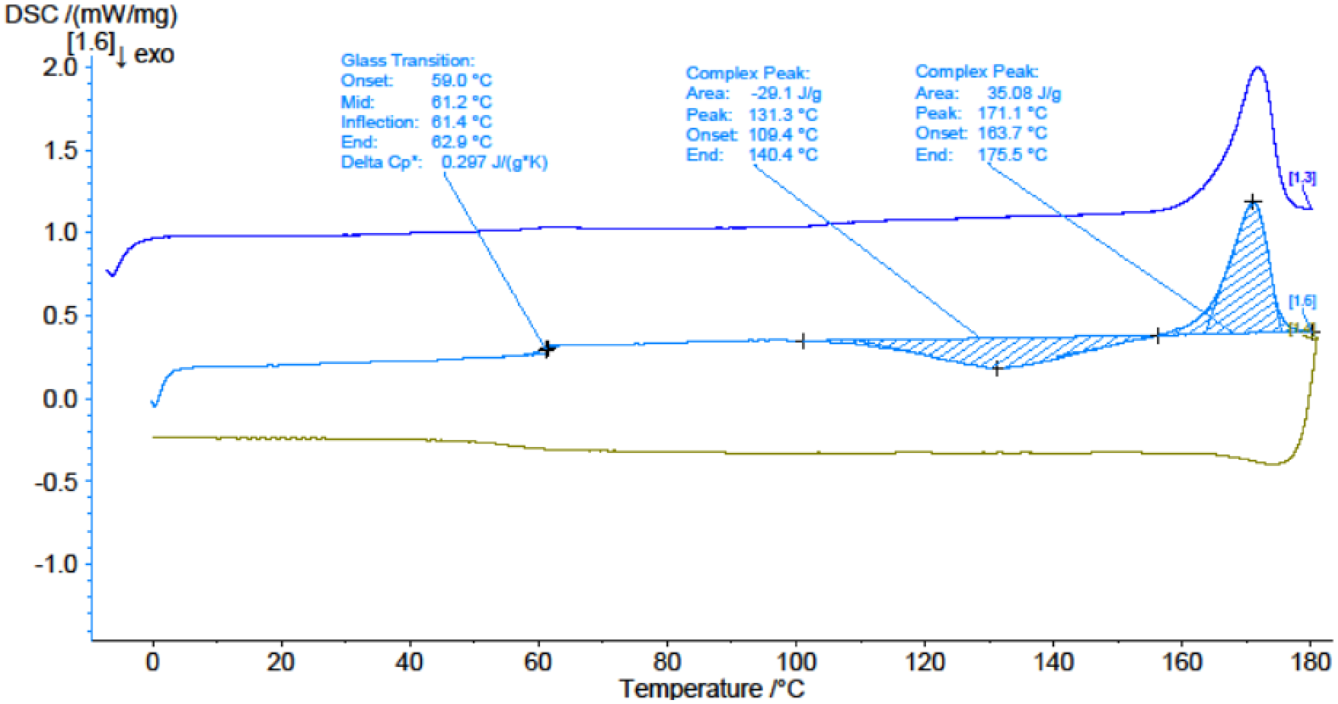

Figure S34. DSC of PS-PLA copolymer (run 1, Table 2).

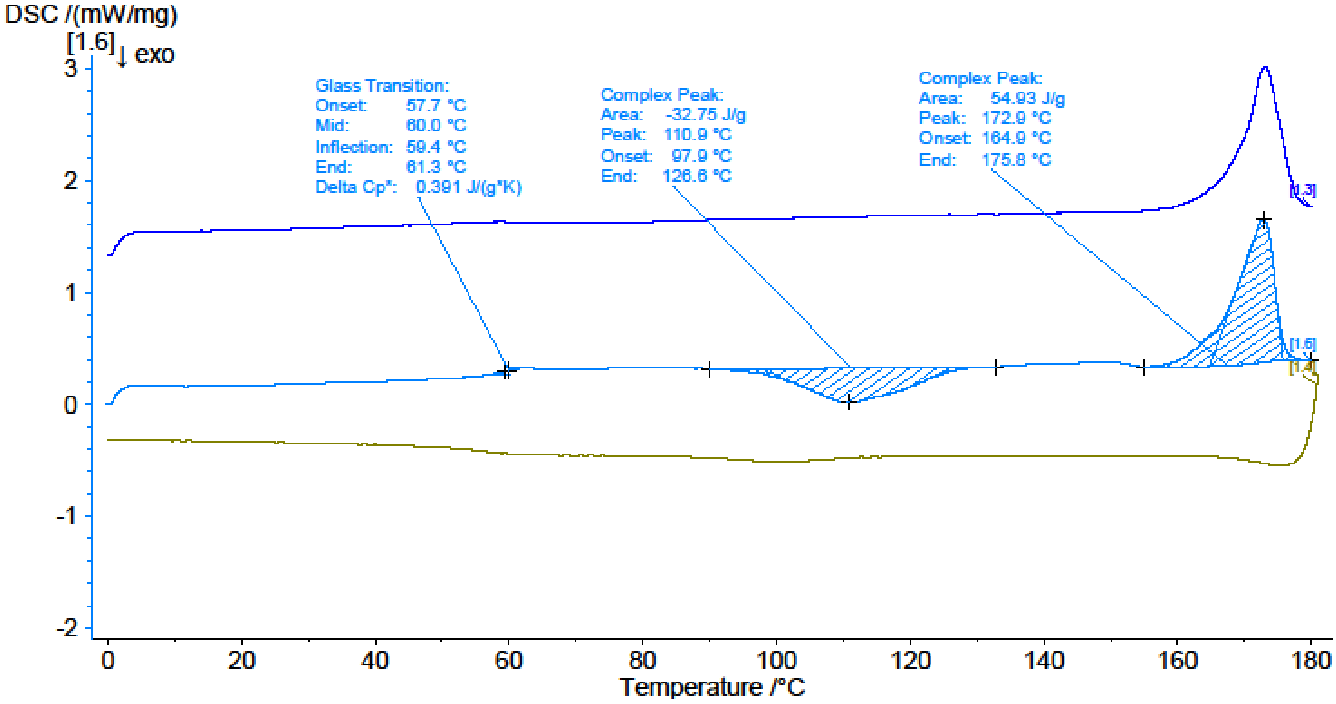

Figure S35. DSC of PS-PLA copolymer (run 2, Table 2).

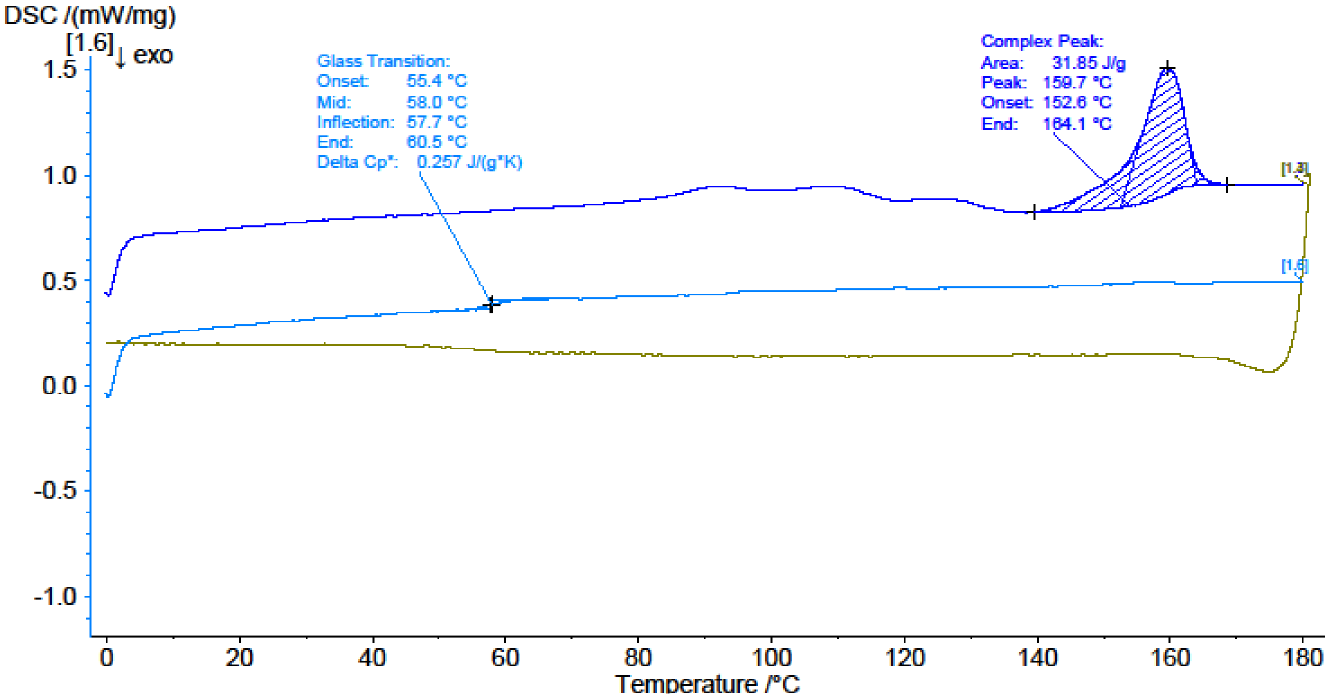

Figure S36. DSC of PS-PLA copolymer (run 3, Table 2).

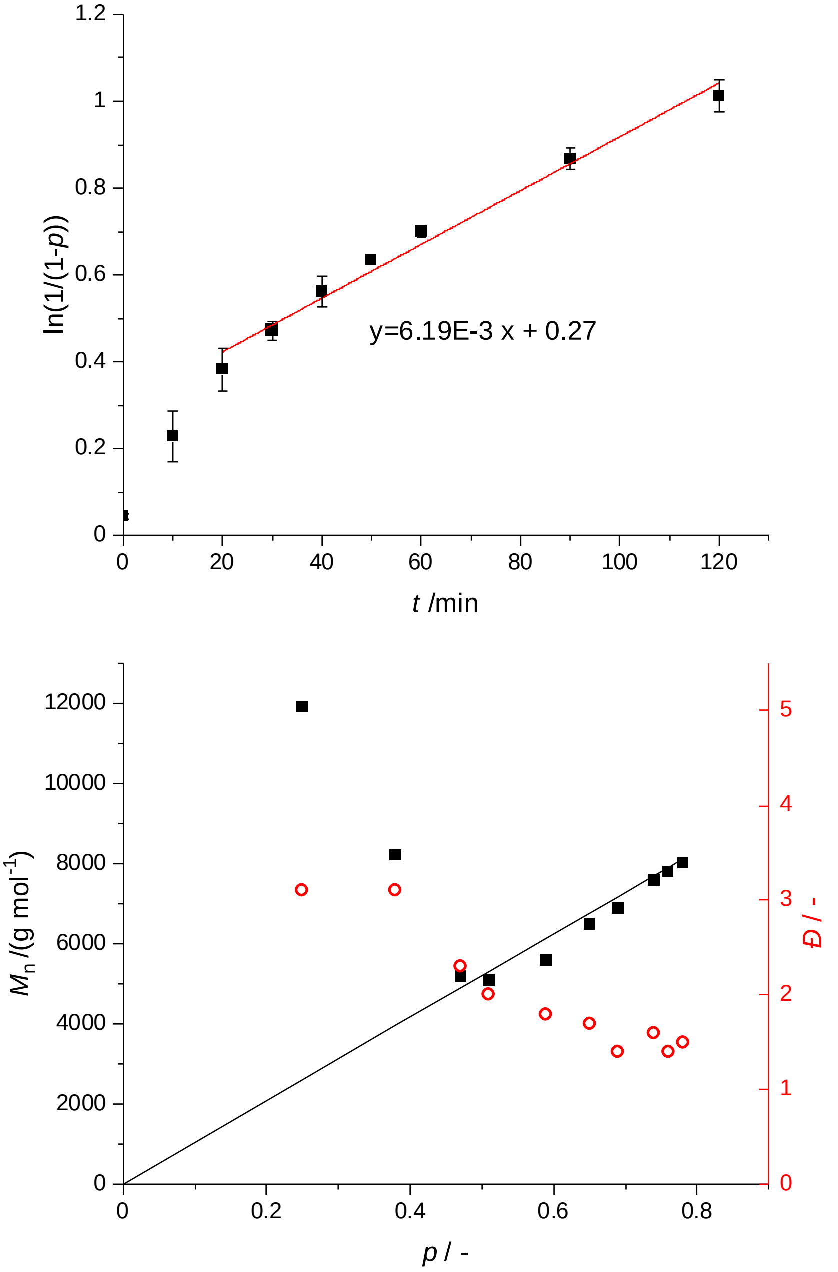

Figure S37. Polymerization of styrene with *in situ* generated **1** with a M/I/Cat ratio of 100:1:1 at 110 °C and 800 rpm under solvent-free conditions. Top: Semilogarithmic plot of conversion *versus* time. Bottom: Theoretical molar masses (black line), experimentally found molar masses (black squares) and dispersities *Đ* (red circles) in the course of the polymerization.

References

[1] J. Leonard, B. Lygo, G. Procter, *Praxis in der organischen Chemie*, VCH-Verlagsgesellschaft, Weinheim, **1996**.

[2] P. Schäfer, M. Fuchs, A. Ohligschläger, R. Rittinghaus, P. McKeown, E. Akin, M. Schmidt, A. Hoffmann, M. Liauw, S. Herres-Pawlis, *ChemSusChem* **2017**, *10*, 3547-3556.

[3] a) *X-Area Pilatus3_SV 1.31.131.0 (STOE, 2017)*; b) *X-Area Recipe 1.33.0.0 (STOE, 2015)*; c) *X-Area Integrate 1.71.0.0 (STOE, 2016)*; d) *X-Area LANA 1.71.4.0 (STOE, 2017)*.

[4] R. D. Rittinghaus, P. M. Schäfer, P. Albrecht, C. Conrads, A. Hoffmann, A. N. Ksiazkiewicz, O. Bienemann, A. Pich, S. Herres-Pawlis, *ChemSusChem* **2019**, *12*, 2161-2165.

[5] L. Yang, D. R. Powell, R. P. Houser, *Dalton Trans.* **2007**, 955-964.

[6] V. Raab, K. Harms, J. Sundermeyer, B. Kovačević, Z. B. Maksić, *J. Org. Chem.* **2003**, *68*, 8790-8797.

[7] E. Fischer, H. J. Sterzel, G. Wegner, *Kolloid Z. Z. Polym.* **1973**, *251*, 980-990.